

## Design and Synthesis of Novel Tricyclic Benzoxazines as Potent 5-HT<sub>1A/B/D</sub> Receptor Antagonists Leading to the Discovery of 6-{2-[4-(2-methyl-5-quinolinyl)-1-piperazinyl]ethyl}-4*H*-imidazo[5,1-*c*][1,4]benzoxazine-3-carboxamide (GSK588045)

Steven M. Bromidge,<sup>\*,†</sup> Roberto Arban,<sup>‡</sup> Barbara Bertani,<sup>‡</sup> Silvia Bison,<sup>‡</sup> Manuela Borriello,<sup>‡</sup> Paolo Cavanni,<sup>‡</sup> Giovanna Dal Forno,<sup>‡</sup> Romano Di-Fabio,<sup>‡</sup> Daniele Donati,<sup>‡,§</sup> Stefano Fontana,<sup>‡</sup> Massimo Gianotti,<sup>‡</sup> Laurie J. Gordon,<sup>†</sup> Enrica Granci,<sup>‡</sup> Colin P. Leslie,<sup>‡</sup> Luca Moccia,<sup>‡</sup> Alessandra Pasquarello,<sup>‡</sup> Ilaria Sartori,<sup>‡</sup> Anna Sava,<sup>‡</sup> Jeannette M. Watson,<sup>†</sup> Angela Worby,<sup>†</sup> Laura Zonzini,<sup>‡</sup> and Valeria Zucchelli<sup>‡</sup>

<sup>†</sup>Neurosciences CEDD, GlaxoSmithKline, New Frontiers Science Park, Third Avenue, Harlow, Essex CM19 5AW, U.K., and

<sup>‡</sup>Medicines Research Centre, Via A. Fleming 4, Verona 37135, Italy. <sup>§</sup>Present address: Nerviano Medical Sciences Srl, Via Pasteur 10, 20014 Nerviano, Milan, Italy.

Received April 20, 2010

Bioisoteric replacement of the metabolically labile *N*-methyl amide group of a series of benzoxazinones with small heterocyclic rings has led to novel series of fused tricyclic benzoxazines which are potent 5-HT<sub>1A/B/D</sub> receptor antagonists with and without concomitant human serotonin transporter (hSerT) activity. Optimizing against multiple parameters in parallel identified 6-{2-[4-(2-methyl-5-quinolinyl)-1-piperazinyl]ethyl}-4*H*-imidazo[5,1-*c*][1,4]benzoxazine-3-carboxamide (GSK588045) as a potent 5-HT<sub>1A/B/D</sub> receptor antagonist with a high degree of selectivity over human ether-à-go-go related gene (hERG) potassium channels, favorable pharmacokinetics, and excellent activity in vivo in rodent pharmacodynamic (PD) models. On the basis of its outstanding overall profile, this compound was progressed as a clinical candidate with the ultimate aim to assess its potential as a faster acting antidepressant/anxiolytic with reduced side-effect burden.

### Introduction

Over the past decades, a wealth of preclinical and clinical evidence has confirmed a link between extracellular levels of serotonin (5-HT) and a plethora of psychiatric indications, in particular anxiety and depression.<sup>1</sup> In fact, enhanced serotonergic neurotransmission has become the unifying mechanism of action of modern day antidepressants and the selective serotonin reuptake inhibitors (SSRIs<sup>6</sup>) have become established as the most effective antidepressant agents in current clinical use.<sup>2</sup> Despite the success of SSRIs, one undesirable characteristic is a long latency to therapeutic onset which is hypothesized to be due to the requirement for desensitization of 5-HT<sub>1</sub> autoreceptors to maintain increased 5-HT levels.<sup>3</sup> This is consistent with preclinical neurochemical studies which have demonstrated that SSRIs such as paroxetine require chronic dosing (14 to 21 days) in order to enhance extracellular 5-HT levels in guinea pig dentate gyrus and rat frontal cortex but have no effect after acute administration.<sup>4</sup>

5-HT<sub>1</sub> autoreceptors are located on both the cell bodies (5-HT<sub>1A</sub>, 5-HT<sub>1B</sub>, and 5-HT<sub>1D</sub> receptor subtypes) and nerve terminals (5-HT<sub>1B</sub> and 5-HT<sub>1D</sub> receptor subtypes) of 5-HT

neurons.<sup>5</sup> They are widely distributed in the brain and in addition to serotonin transporters (SerT) are known to have a major role in the control of synaptic 5-HT levels.<sup>5</sup> Blockade of 5-HT<sub>1A/B/D</sub> autoreceptors, with or without concomitant SerT inhibition, rapidly increases brain 5-HT levels and consequently should provide a fast onset of antidepressant/anxiolytic action relative to current therapies.<sup>6</sup>

We have previously reported several series of potent 5-HT<sub>1A/B/D</sub> receptor antagonists both with and without additional hSerT reuptake inhibitory activity including **1** (SB-649915) (Figure 1).<sup>7</sup> More recently we disclosed a series of 6- and 8-[2-(4-aryl-1-piperazinyl)ethyl]-2*H*-1,4-benzoxazin-3(4*H*)-ones with interesting in vitro and in vivo profiles (such as **2–5**).<sup>8,9</sup> This article reports the further optimization and evolution of these compounds which has resulted in the identification of novel series of tricyclic benzoxazines culminating in the identification of **20** (GSK588045). This compound demonstrated an outstanding overall profile with in vivo activity in different animal models of anxiety and depression and has been progressed as a clinical candidate.

**Chemistry.** The synthesis of the 6-substituted (**2** and **3**) and 8-substituted (**4** and **5**) compounds has been previously described.<sup>8,9</sup> The unsubstituted 4*H*-imidazo[2,1-*c*][1,4]benzoxazine **6** was prepared as shown in Scheme 1. Thus, 8-(2-propen-1-yl)-2*H*-1,4-benzoxazin-3(4*H*)-one<sup>9</sup> **30** was converted into the 3-(methylthio)-2*H*-1,4-benzoxazine **32** via the corresponding thione **31**. Reaction of **32** with amino acetaldehyde dimethyl acetal afforded the aminoacetal **33**, which readily cyclized to the desired 6-(2-propen-1-yl)-4*H*-imidazo[2,1-*c*][1,4]benzoxazine **34** on heating with HCl.

\*To whom correspondence should be addressed. Phone: +44 (0)1279 627031. Fax: +44 (0)1279 622371. E-mail: stevebromidge@gmail.com.

<sup>6</sup>Abbreviations: hSerT, human serotonin transporter; hERG, human ether-à-go-go related gene; SSRIs, selective serotonin reuptake inhibitors; SAR, structure–activity relationships; PD, pharmacodynamic; PK, pharmacokinetic; TI, therapeutic index; LHS, left-hand side; IA, intrinsic activity; CYP450, cytochrome P450; DDI, drug–drug interactions; V<sub>ss</sub>, volumes of distribution; HEK, human embryo kidney; GSH, glutathione; CHO, Chinese hamster ovary.

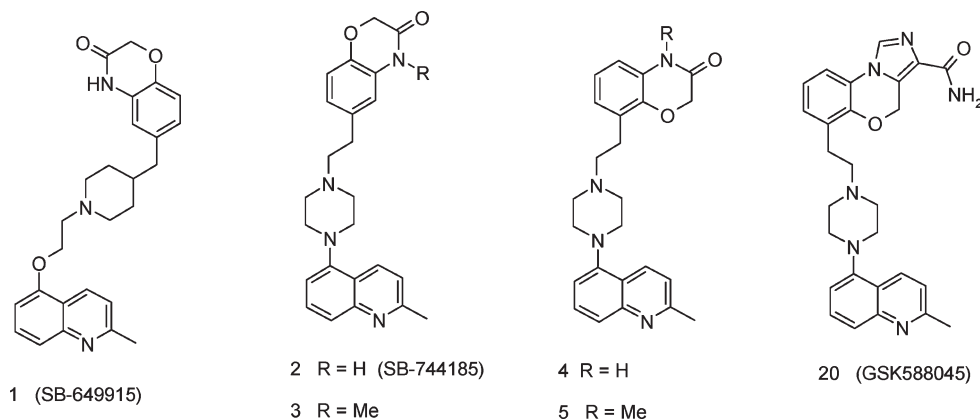
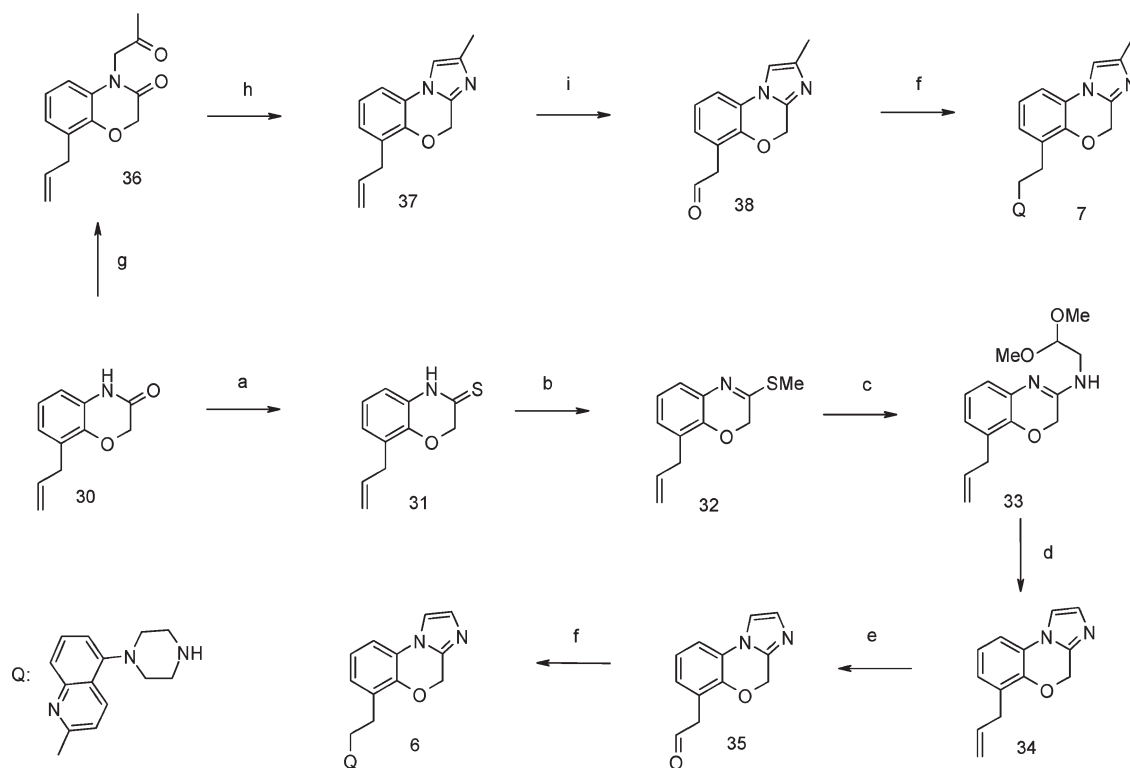


**Figure 1.** Chemical structures of different series of 5-HT<sub>1A/B/D</sub> antagonists.

**Scheme 1.** Synthetic Route for Compounds **6** and **7**<sup>a</sup>



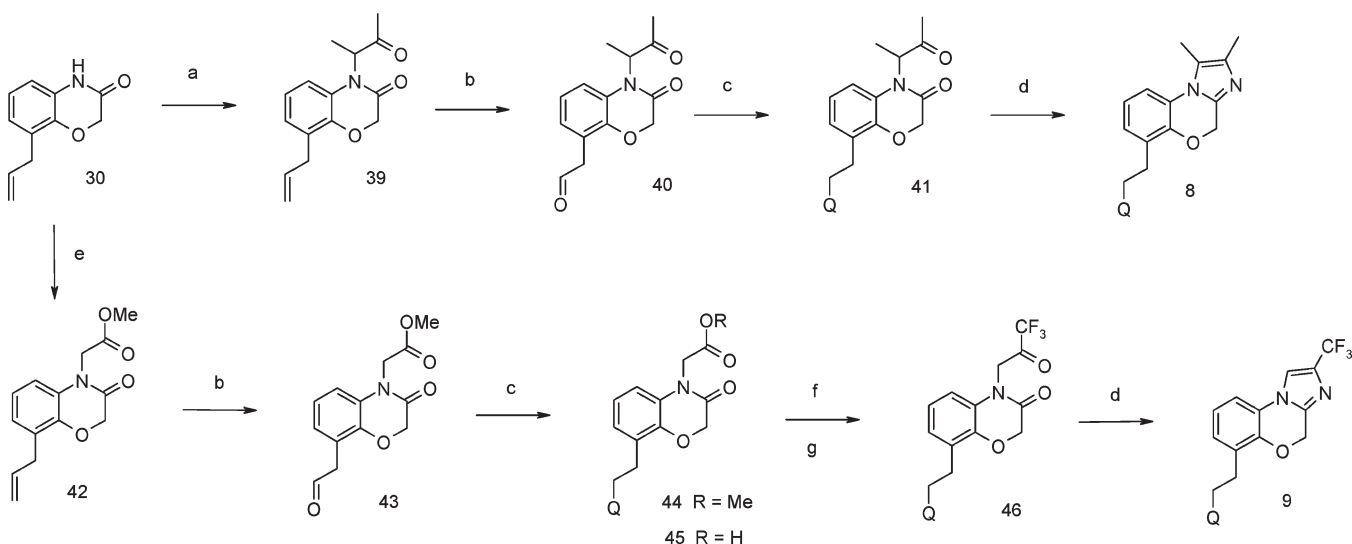
<sup>a</sup> (a) Lawesson's reagent, toluene, reflux, 1 h; (b) MeI, KOH, acetone, reflux, 2 h; (c) NH<sub>2</sub>CH<sub>2</sub>CH(OMe)<sub>2</sub>, EtOH, reflux, 9 h; (d) conc HCl, MeOH, reflux, 3 h; (e) (i) OsO<sub>4</sub>, 4-methylmorpholine *N*-oxide, acetone/H<sub>2</sub>O, room temp, 36 h; (ii) aq Na<sub>2</sub>SO<sub>3</sub>, room temp, 30 min; (f) 2-methyl-5-piperazin-1-ylquinoline, 1,2-dichloroethane, NaB(OAc)<sub>3</sub>H, room temp, 3 h; (g) NaH, 1-chloro-2-propanone, DMF, 0 °C to room temp, 7 h; (h) NH<sub>4</sub>OAc, AcOH, microwave 150 °C, 10 min; (i) OsO<sub>4</sub>, NaIO<sub>4</sub>, THF/water, room temp, 2 h.

Oxidative cleavage of the pendant vinyl of **34** with osmium tetroxide/sodium periodate to the aldehyde **35** followed by reductive amination with 2-methyl-5-(1-piperazinyl)quinoline completed the synthesis. The 2-methyl analogue **7** was similarly prepared from **30** but by an alternative cyclization strategy via the ketone **36** which was condensed with ammonium acetate to **37**, followed by oxidative cleavage of the vinyl and reductive amination as above to afford **7** (Scheme 1).

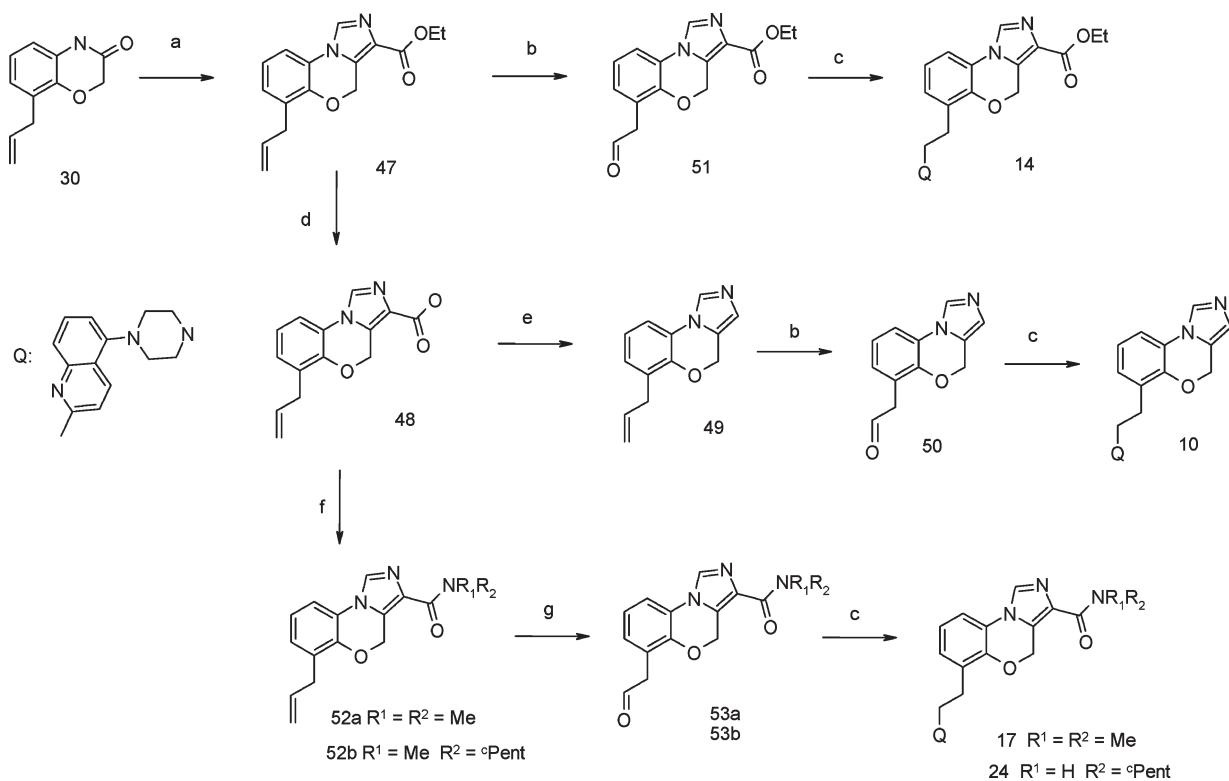
The 1,2-dimethyl **8** and 2-trifluoromethyl **9** 4*H*-imidazo[2,1-*c*][1,4]benzoxazine analogues were also prepared indirectly from **30** via the corresponding ketones **39** and **46**, respectively, as described above for **7** except that cyclization of the imidazole ring was carried out as the final steps (Scheme 2).

The unsubstituted 4*H*-imidazo[5,1-*c*][1,4]benzoxazine **10** was also prepared from the key intermediate **30** as shown in Scheme 3. Thus, treatment of **30** with diethyl chlorophosphate and potassium *t*-butoxide followed by ethyl isocyanacetate smoothly afforded the 4*H*-imidazo[5,1-*c*][1,4]-benzoxazine-3-ethylcarboxylate **47**.<sup>10</sup> Saponification gave the acid **48**, which was decarboxylated to **49** and converted to the desired product **10** as described above. The acid **48** also served as a key intermediate for the preparation of the amides **17** and **24**. The 4*H*-imidazo[5,1-*c*][1,4]benzoxazine-3-ethylcarboxylate **47** was itself converted to the final compound **14** (Scheme 3).

To rapidly investigate the amidic portion of this class of compounds, a slightly modified route was set up starting from the advanced ester intermediate **14** (Scheme 4): amides **17**,

Scheme 2. Synthetic Route for Compounds 8 and 9<sup>a</sup>

<sup>a</sup> (a) 3-Chloro-2-butanone, K<sub>2</sub>CO<sub>3</sub>, acetone, reflux, 4 h; (b) OsO<sub>4</sub>, NaIO<sub>4</sub>, THF/water, room temp, 2 h; (c) 2-methyl-5-piperazin-1-ylquinoline, 1,2-dichloroethane, NaB(OAc)<sub>3</sub>H, room temp, 3 h; (d) NH<sub>4</sub>OAc, AcOH, microwave 150 °C, 10 min; (e) NaH, methyl bromoacetate, DMF, 0 °C to room temp, 6 h; (f) NaOH, MeOH, room temp, 4 h; (g) (i) oxalyl chloride, DMF, toluene, 60 °C, 3 h; (ii) trifluoroacetic anhydride, pyridine, room temp, 2 h.

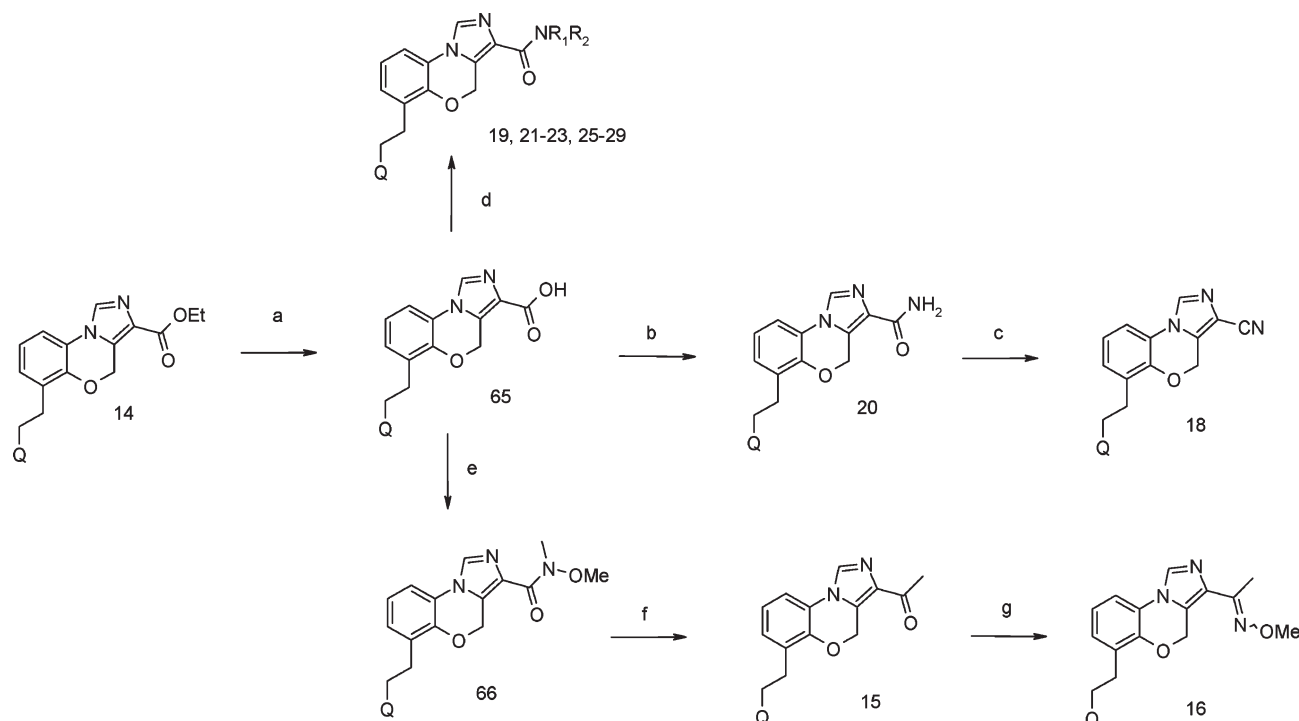
Scheme 3. Synthetic Route for Compounds 10, 14, 17, and 24<sup>a</sup>

<sup>a</sup> (a) KO<sup>t</sup>Bu, diethyl chlorophosphate, DMF, 0 °C, 10 min then ethyl isocyanacetate, 60 °C, 6 h; (b) OsO<sub>4</sub>, NaIO<sub>4</sub>, THF/water, room temp, 2 h; (c) 2-methyl-5-piperazin-1-ylquinoline, 1,2-dichloroethane, NaB(OAc)<sub>3</sub>H, room temp, 3 h; (d) NaOH, MeOH, 60 °C, 30 min; (e) 1,2-dichlorobenzene, microwave 250 °C, 10 min; (f) HOBT, EDC, NHR<sub>1</sub>R<sub>2</sub>, DMF/CH<sub>2</sub>Cl<sub>2</sub>, room temp, 4 h; (g) (i) OsO<sub>4</sub>, 4-methylmorpholine *N*-oxide, acetone/H<sub>2</sub>O, room temp, 36 h; (ii) NaIO<sub>4</sub>, THF/H<sub>2</sub>O, room temp, 1 h.

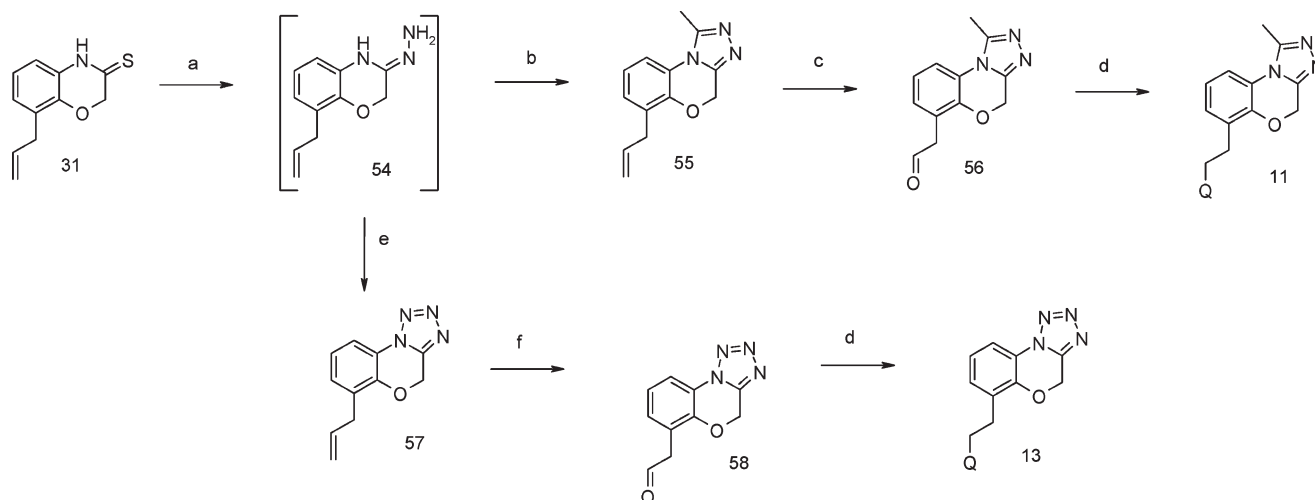
19–23, 25–29 were obtained via the acid 65 by standard coupling methods. In addition, the methyl ketone 15 and oxime 16 were prepared via the Weinreb amide 66, while the nitrile 18 was obtained via the corresponding primary amide 20.

The next step of the exploration was directed to the investigation of different fused heterocyclic moieties. Thus, the 1-methyl-4*H*-[1,2,4]triazolo[3,4-*c*][1,4]benzoxazine 11 and the

4*H*-tetrazolo[5,1-*c*][1,4]benzoxazine 13 were prepared starting from the benzoxazine-3(4*H*)-thione 31 prepared as described above. Thus, 31 was converted to the hydrazone 54, which was treated with trimethyl orthoacetate or sodium nitrite respectively to afford the triazole 55 or the tetrazole 57, which were then converted by the methods described above to the final compounds 11 and 13, respectively (Scheme 5).

**Scheme 4.** Synthetic Route for Compound **15–16**, **18–19**, **21–23**, and **25–29**<sup>a</sup>

<sup>a</sup> (a) NaOH, MeOH/H<sub>2</sub>O, microwave 120 °C, 5 min; (b) DIPEA, TBTU, hexamethyldisilazane, DMF, room temp, 1 h; (c) (CF<sub>3</sub>)<sub>2</sub>CO, pyridine/THF, 0 °C, 1 h; (d) DIPEA, TBTU, NHR<sub>1</sub>R<sub>2</sub>, DMF, room temp, 1 h; (e) DIPEA, TBTU, NHMeOMe·HCl, DMF, room temp, 1 h; (f) MeMgBr, THF, 0 °C, 1 h; (g) NH<sub>2</sub>OMe·HCl, pyridine/EtOH, reflux, 2 h.

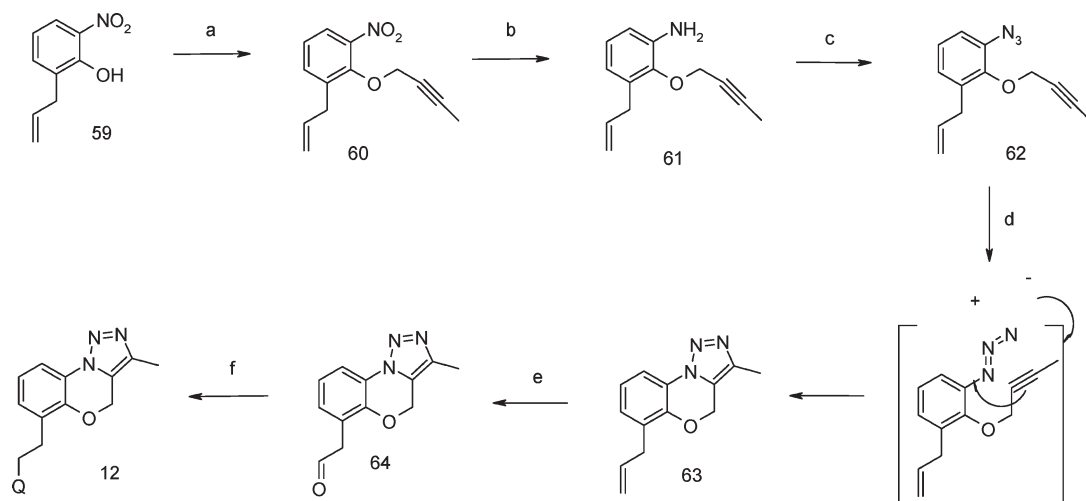
**Scheme 5.** Synthetic Route for Compounds **11** and **13**<sup>a</sup>

<sup>a</sup> (a) NH<sub>2</sub>NH<sub>2</sub>·H<sub>2</sub>O, EtOH, 80 °C, 2 h; (b) MeC(OMe)<sub>3</sub>, microwave 150 °C, 10 min; (c) (i) OsO<sub>4</sub>, 4-methylmorpholine *N*-oxide, acetone/H<sub>2</sub>O, room temp, 36 h; (ii) NaIO<sub>4</sub>, THF/H<sub>2</sub>O, room temp, 1 h; (d) 2-methyl-5-(1-piperazinyl)quinoline, 1,2-dichloroethane, NaB(OAc)<sub>3</sub>H, room temp, 3 h; (e) NaNO<sub>2</sub>, aq HCl, 5 °C, 4 h; (f) OsO<sub>4</sub>, NaIO<sub>4</sub>, THF/water, room temp, 2 h.

An elegant route was established to the 1,2,3-triazole **12** starting with alkylation of 2-nitro-6-(2-propen-1-yl)phenol **59** with 1-bromo-2-butyne followed by functional group transformation of the nitro to the azide **62**. Heating the azide **62** gave smooth intramolecular 1,3-dipolar cycloaddition, generating the tricyclic system **63** in a single step.<sup>11</sup> Oxidative cleavage and reductive amination with 2-methyl-5-(1-piperazinyl)quinoline according to the general procedures described above completed the synthesis (Scheme 6).

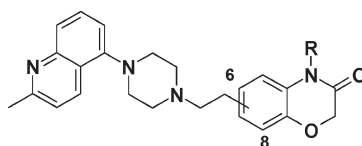
## Results and Discussion

We recently disclosed a series of 6-[2-(4-aryl-1-piperazinyl)ethyl]-2*H*-1,4-benzoxazin-3(4*H*)-ones as potent 5-HT<sub>1A/B/D</sub> receptor antagonists, a number of which had additional hSerT reuptake inhibitory activity (Table 1).<sup>8</sup> Modulation of the balance between the different target affinities allowed us to identify compounds with interesting *in vitro* and *in vivo* profiles. Unfortunately, the progression of these molecules was precluded by the finding that they had significant inhibitory activity at hERG potassium channels which has been

Scheme 6. Synthetic Route for Compound 12<sup>a</sup>

<sup>a</sup> (a) K<sub>2</sub>CO<sub>3</sub>, 1-bromo-2-butyne, acetone, reflux, 4 h; (b) Fe powder, AcOH, room temp, 16 h; (c) (i) NaNO<sub>2</sub>, aq HCl, 0 °C, 30 min; (ii) NaN<sub>3</sub>, H<sub>2</sub>O, 5 °C, 30 min; (d) toluene, reflux, 2.5 h; (e) OsO<sub>4</sub>, NaIO<sub>4</sub>, THF/water, room temp, 2 h; (f) 2-methyl-5-piperazin-1-ylquinoline, 1,2-dichloroethane, NaB(OAc)<sub>3</sub>H, room temp, 3 h.

**Table 1.** Functional Activity (*f*-pK<sub>i</sub> or pEC<sub>50</sub>)<sup>a,b</sup> for Human 5-HT<sub>1A/B/D</sub> Receptors with Intrinsic Activity (IA), hSerT and hERG Binding Affinities (pK<sub>i</sub>)<sup>b</sup> and Rat PK Parameters for Benzoxazinones (2–5)



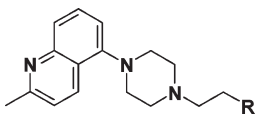
compd	sub	R	<i>f</i> -pK <sub>i</sub> or *pEC <sub>50</sub> <sup>a,b</sup>			pK <sub>i</sub> <sup>b</sup>		rat PK parameters <sup>d</sup>					
			5-HT <sub>1A</sub> (IA)	5-HT <sub>1B</sub> (IA)	5-HT <sub>1D</sub> (IA)	hSerT	hERG	Cli rat; hum <sup>c</sup>	mL/min/g liver	CLb mL/min/kg	V <sub>ss</sub> L/kg	t <sub>1/2</sub> h	Fpo %
2	6	H	10.2 (0.0)	6.6 (0.0)	*9.3 (0.6)	8.9	7.2	1.3; <0.5	5	2.0	5.1	68	1.6
3		Me	10.1 (0.3)	8.7 (0.3)	10.0 (0.0)	7.7	6.1	0.8; 1.1	8	2.7	4.4	59	2.2
4	8	H	9.6 (0.0)	9.0 (0.0)	10.3 (0.0)	6.5	5.6	0.7; 1.0	8	3.4	5.2	63	0.7
5		Me	9.8 (0.0)	8.4 (0.0)	9.5 (0.0)	8.0	5.4	1.0; 2.4	29	1.7	1.0	26	1.5

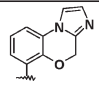
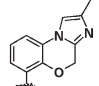
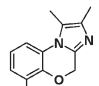
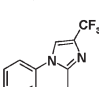
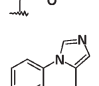
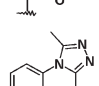
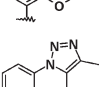
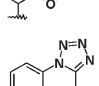
<sup>a</sup>Data from the agonist mode (pEC<sub>50</sub>)<sup>a</sup> are reported for those compounds with intrinsic activity (IA) ≥ 0.4 in this mode (i.e., partial or full agonists), whereas, for those compounds with IA < 0.4 in the agonist mode (i.e., antagonists), data from the antagonist mode is reported (*f*-pK<sub>i</sub>). See Experimental Section for assay details. <sup>b</sup>Each determination lies within 0.3 log units of the mean with a minimum of 3 replicates. See Experimental Section for assay details. <sup>c</sup>Intrinsic clearance in liver microsomes. See Experimental Section for assay details. <sup>d</sup>In vivo data determined by 0.5 mg/kg iv and 1 mg/kg po administration in rat. Br:Bl at 1 h following iv dosing.

associated with increases in the QT interval prolongation and the induction of potentially life-threatening ventricular arrhythmias in the clinic (Torsades de Pointes).<sup>12</sup> For example, 2 had pK<sub>i</sub> of 7.2 in a hERG binding assay which translated to potent functional inhibition of hERG tail current in whole cell electrophysiology studies.<sup>13</sup> Interestingly, the corresponding NMe analogue 3 showed 10-fold reduced hERG affinity relative to 2 despite increased lipophilicity, which was somewhat surprising since lipophilicity has been positively correlated with hERG.<sup>14</sup> This finding led us to speculate a specific binding interaction between the lactam N–H and the hERG channel, and we subsequently discovered that transposing the substitution point of the linker from the 6- to the 8-position of the benzoxazinone ring selectively disrupted binding to the hERG channel while maintaining the key target interactions.<sup>9</sup> Thus, the 8-substituted analogues 4 and 5 were found to have similar or improved pan 5-HT<sub>1A/B/D</sub> antagonist potencies relative to 2 and 3 with significantly reduced hERG affinities (40- and 5-fold, respectively). Of particular note, the structure–activity relationships (SAR) for hSerT was reversed with respect to the 6-substituted series, and whereas the 6-substituted NH analogue 2 demonstrated 15-fold higher hSerT affinity than the

corresponding NMe analogue 3, the 8-substituted NH analogue 4 showed 30-fold lower hSerT affinity compared to the corresponding NMe analogue 5.

Although 4 and 5 possessed interesting and distinct pharmacological profiles (additional hSerT component in the case of 5) of potential therapeutic utility with reduced hERG/QT risk, pharmacokinetic (PK) studies revealed nonideal in vivo profiles. Thus, in rat PK studies (Table 1), 4 demonstrated high oral bioavailability combined with low blood clearance, a good half-life, but a relatively modest brain to blood ratio (0.7). In contrast, the corresponding *N*-methyl analogue 5 achieved a higher brain to blood ratio (1.5) and good brain exposures but was more rapidly cleared than 4, resulting in modest half-life and bioavailability. Further investigation determined that *N*-demethylation was a principle route of metabolism in rat as evidenced by the detection of high circulating levels of the des-methyl analogue 4 following oral dosing of 5. In addition, the observation that 5 was also efficiently converted to 4 in vitro in the presence of both rat and human liver microsomes with a higher intrinsic clearance, with the latter suggested a potentially higher rate of metabolism in man.

**Table 2.** Functional Activity ( $f$ -pK<sub>i</sub> or pEC<sub>50</sub>)<sup>a,b</sup> for Human 5-HT<sub>1A/B/D</sub> Receptors with Intrinsic Activity (IA), hSerT and hERG Binding Affinities (pK<sub>i</sub>),<sup>b</sup> Microsomal Intrinsic Clearance and Human CYP450 Activity for Tricyclobenzoxazines (**6–13**)


Cmpd	R	$f$ -pK <sub>i</sub> <sup>a,b</sup>			pK <sub>i</sub> <sup>b</sup>		CYP450 <sup>c</sup> IC <sub>50</sub> (μM)	Cli rat; hum <sup>d</sup> ml/min/g liver
		5-HT <sub>1A</sub> (I.A.)	5-HT <sub>1B</sub> (I.A.)	5-HT <sub>1D</sub> (I.A.)	hSerT	hERG		
6		9.9 (0.0)	8.8 (0.0)	10.0 (0.0)	7.7	5.8	2C9, 2C19; 4	3.6; 4.1
7		9.7 (0.0)	8.8 (0.0)	9.9 (0.0)	7.7	6.4	2C9, 3A4(DEF); < 4	4.1; 3.0
8		9.7 (0.0)	8.7 (0.0)	9.8 (0.0)	7.8	6.4	2C9, 3A4(DEF); < 4	7.6; 6.6
9		9.8 (0.0)	9.0 (0.0)	9.9 (0.0)	7.5	7.6	2C9, 3A4(DEF); < 4	0.6; 1.1
10		9.7 (0.0)	9.0 (0.0)	9.9 (0.0)	7.9	6.0	1A2, 2C9; < 2 2C19, 2D6; < 1 3A4(DEF/7BQ); 0.1	1.0; 2.1
11		10.1 (0.0)	9.1 (0.0)	9.8 (0.0)	6.7	4.9	All > 10	0.5; 1.8
12		10.1 (0.0)	8.6 (0.0)	9.9 (0.0)	8.0	5.6	All > 5	<0.5; 1.4
13		9.3 (0.0)	8.1 (0.0)	9.9 (0.0)	7.3	6.3	1A2; 1	<0.5; 1.3

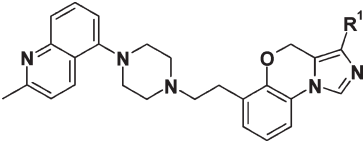
<sup>a</sup>Data from the agonist mode (pEC<sub>50</sub>)<sup>a</sup> are reported for those compounds with intrinsic activity (IA) ≥ 0.4 in this mode (i.e., partial or full agonists), whereas for those compounds with IA < 0.4 in the agonist mode (i.e., antagonists), data from the antagonist mode is reported ( $f$ -pK<sub>i</sub>). See Experimental Section for assay details. <sup>b</sup>Each determination lies within 0.3 log units of the mean with a minimum of 3 replicates. See Experimental Section for assay details. <sup>c</sup>CYP450 assay: IC<sub>50</sub> ≥ 5 μM against different isoforms unless stated. See Experimental Section for assay details. <sup>d</sup>Intrinsic clearance in liver microsomes. See Experimental Section for assay details.

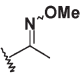
As a result of the above findings, we designed and implemented medicinal chemistry strategies aimed at circumventing metabolic amide dealkylation of **5** with the ultimate objective of identifying potent metabolically stable and brain penetrant 5-HT<sub>1A/B/D</sub> receptor antagonists with or without additional hSerT reuptake inhibitory activity together with further increased therapeutic index (TI) over hERG. Several approaches were investigated to this end including modification of the nature of the *N*-alkyl group and modulation of the electronic properties of the benzoxazinone system, but the most successful tactic proved to be incorporation of the amide *N*-methyl into a fused heterocyclic ring.

We initially targeted a range of tricyclic fused heterocycles based on electrostatic potential similarity to **5** in combination with chemical feasibility. This exploration was undertaken with the left-hand side (LHS) of the molecule fixed as the 5-(4-ethyl-1-piperazinyl)-2-methylquinoline since we had previously found that this conferred a favorable overall balance of properties and in particular afforded low intrinsic activity (IA) at 5-HT<sub>1A/B/D</sub> receptors.<sup>8</sup> Encouragingly, a number of new heterotricyclic ring systems rapidly emerged with interesting profiles

such as the fused imidazo, triazolo, and tetrazolo-benzoxazines (**6–12**). The isomeric 1,2- and 1,5-fused imidazobenzoxazines (**6** and **10**) demonstrated similar target profiles to **5**, displaying excellent 5-HT<sub>1A/B/D</sub> antagonist potencies and moderate hSerT affinity (Table 2). However, the hERG affinities and the microsomal human intrinsic clearances were similar or increased relative to **5**. In addition, significant human cytochrome P450 (CYP450) inhibitory activities emerged, particularly in the case of **10**, indicating a high risk of potential drug–drug interactions (DDI) in a clinical setting.<sup>15</sup>

The 1,3,4- and 1,2,3-triazoles (**11** and **12**) showed increased 5-HT<sub>1A/B/D</sub> antagonist potencies together with clean CYP450 profiles and reduced intrinsic clearance in rat and human microsomes compared to **5** (Table 2). Whereas **12** had similar hSerT and hERG affinities to **5**, compound **11** had reduced affinities at both. On the basis of the increased separation between 5-HT<sub>1A/B/D</sub> potencies and hERG, **11** was progressed to rat PK studies (Table 5). Encouragingly, the lower microsomal clearance translated to reduced *in vivo* clearance and increased oral bioavailability and half-life relative to **5**, although the brain to blood ratio was significantly reduced.

**Table 3.** Functional Activity ( $f$ -p*K<sub>i</sub>* or pEC<sub>50</sub>)<sup>a,b</sup> for human 5-HT<sub>1A/B/D</sub> Receptors with Intrinsic Activity (IA), hSerT and hERG binding affinities (p*K<sub>i</sub>*),<sup>b</sup> Microsomal Intrinsic Clearance and Human CYP450 Activity for 3-Substituted-4*H*-imidazo[5,1-*c*][1,4]benzoxazines (**14–18**)


Cmpd	R <sup>1</sup>	$f$ -p <i>K<sub>i</sub></i> <sup>a,b</sup>			p <i>K<sub>i</sub></i> <sup>b</sup>		CYP450 <sup>c</sup> IC <sub>50</sub> (μM)	Cli rat; hum <sup>d</sup> ml/min/g liver
		5-HT <sub>1A</sub> (I.A.)	5-HT <sub>1B</sub> (I.A.)	5-HT <sub>1D</sub> (I.A.)	hSerT	hERG		
<b>10</b>	H	9.7 (0.0)	9.0 (0.0)	9.9 (0.0)	7.9	6.0	1A2, 2C9; < 2 2C19, 2D6; < 1 3A4(DEF/7BQ); 0.1	1.0; 2.1
<b>14</b>	CO <sub>2</sub> Et	9.2 (0.0)	8.9 (0.0)	9.5 (0.0)	7.8	5.1	2C9; 4	0.6; 1.5
<b>15</b>	COMe	9.5 (0.0)	9.0 (0.0)	10.0 (0.0)	7.5	5.2	All > 5	0.5; 1.0
<b>16</b>		8.8 (0.0)	8.6 (0.0)	9.5 (0.0)	7.4	5.6	1A2, 2C9; 4	0.7; 1.7
<b>17</b>	CONMe <sub>2</sub>	9.8 (0.0)	9.2 (0.0)	9.8 (0.0)	7.8	5.4	All > 10	0.5; 1.6
<b>18</b>	CN	9.0 (0.0)	8.8 (0.0)	8.7 (0.0)	6.9	6.0	2C9; 2 3A4(DEF/7BQ); 4	<0.5; 1.3

<sup>a</sup> Data from the agonist mode (pEC<sub>50</sub>)<sup>\*</sup> are reported for those compounds with intrinsic activity (IA) ≥ 0.4 in this mode (i.e., partial or full agonists), whereas for those compounds with IA < 0.4 in the agonist mode (i.e., antagonists), data from the antagonist mode is reported ( $f$ -p*K<sub>i</sub>*). See Experimental Section for assay details. <sup>b</sup> Each determination lies within 0.3 log units of the mean with a minimum of 3 replicates. See Experimental Section for assay details. <sup>c</sup> CYPEX assay: IC<sub>50</sub> ≥ 5 μM against different isoforms unless stated. See Experimental Section for assay details. <sup>d</sup> Intrinsic clearance in liver microsomes. See Experimental Section for assay details.

The fused tetrazolo-benzoxazine **13** also maintained a good overall target profile together with low intrinsic clearance although 5-HT<sub>1A</sub>, 5-HT<sub>1B</sub>, and hSerT potencies were somewhat reduced relative to **5** and a significant increase in hERG affinity was evident (Table 2). The increased hERG affinity of **13** (and the 1,2,3-triazole **12**) compared to the 2-methyltriazole **11** is suggestive of a specific H-bond interaction between the additional nitrogen in the tetrazole ring system and the hERG channel.

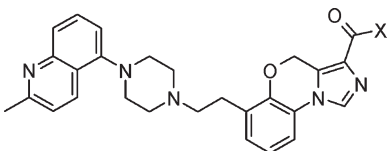
On the basis of the above promising results, the fused imidazobenzoxazines (**6** and **10**) were selected for further optimization and the introduction of different substituents into key positions of the imidazole rings was undertaken with the aim of increasing metabolic stability by blocking putative sites of metabolism and reducing CYP450 interactions. Substitution of the 4 and 5 position of the fused 1,2-imidazobenzoxazine system with methyl (**8** and **7**) maintained target potencies but increased hERG with no reduction in intrinsic clearance. The 4-trifluoromethyl analogue **9** did show significantly reduced intrinsic clearance combined with a promising target profile but at the cost of dramatically increased hERG affinity.

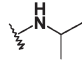
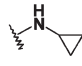
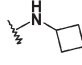
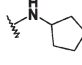
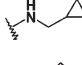
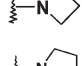
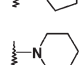
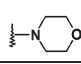
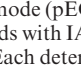
The 3 position of the fused 1,5-imidazo-benzoxazine **10** was hypothesized to be a site of potential metabolism, and therefore the introduction of small electron withdrawing groups such as nitrile, ketones, and amides was undertaken in order to reduce lipophilicity with the aim of addressing both the clearance and CYP450 issues and further increasing selectivity over hERG. Encouragingly, the ethyl ester **14**, methyl ketone **15**, ketoxime ether **16**, and the dimethyl amide **17** all maintained very similar target profiles across 5-HT<sub>1A/B/D</sub> and hSerT compared to **10** but demonstrated significantly reduced hERG affinity together with reduced intrinsic clearance and favorable CYP450 inhibitory profiles (Table 3). The cyano derivative **18**

also maintained a good overall profile, although hSerT affinity and selectivity between 5-HT<sub>1A/B/D</sub> and hERG were reduced.

On the basis of their favorable in vitro profiles, **15**, **17**, and **18** were evaluated in rat PK studies (Table 5). Whereas **17** had comparable in vivo clearance to **5**, in the case of **15** and **18**, the lower microsomal clearance translated to reduced in vivo clearance and, in combination with increased volumes of distribution (V<sub>ss</sub>), afforded significant increases in terminal half-life. All three imidazobenzoxazines demonstrated good bioavailability and favorable brain to blood ratios (consistent with higher V<sub>ss</sub>). In an attempt to explain the disconnect between the rat in vitro and in vivo clearance for **17**, we hypothesized that the dimethyl amide may be subject to metabolic demethylation in vivo. This putative route of metabolism was supported by the detection of high levels of a (M<sup>+</sup>-14) metabolite in rat PK samples and led us to prepare a series of amide analogues including cyclic tertiary amides (**26–29**), secondary amides (**19**, **21–25**) and the primary amide **20** (Table 4).

The secondary *N*-methyl amide **19** had an excellent overall in vitro profile which was similar to that of **17** but with even further reduced hERG affinity. Increasing the size and lipophilicity of the secondary *N*-alkyl substituent (**21–25**) maintained exquisitely high 5-HT<sub>1A/B/D</sub> antagonist potencies and afforded modest gains in hSerT but with concomitant increases in hERG affinities and increased intrinsic clearance (particularly by human microsomes). The 4, 5, and 6-membered cyclic tertiary amides (**26–28**) also maintained impressive 5-HT<sub>1A/B/D</sub> antagonist potencies together with increased hSerT and hERG affinities, which, as above, was consistent with increased lipophilicity. The morpholino analogue **29** was of particular interest, affording the lowest hERG affinity yet observed in this series and low CYP450 inhibitory potencies together with low intrinsic clearance. In addition, **29** displayed subnanomolar antagonist potencies against 5-HT<sub>1A/B/D</sub> receptors even though

**Table 4.** Functional Activity ( $f$ - $pK_i$  or  $pEC_{50}$ )<sup>a,b</sup> for Human 5-HT<sub>1A/B/D</sub> Receptors with Intrinsic Activity (IA), hSerT and hERG Binding Affinities ( $pK_i$ ),<sup>b</sup> Microsomal Intrinsic Clearance and Human CYP450 Activity for 3-Amido-4H-imidazo[5,1-c][1,4]benzoxazines (**19–29**)


Cmpd	X	$f$ - $pK_i$ <sup>a,b</sup>			$pK_i$ <sup>b</sup>		CYP450 <sup>c</sup> IC <sub>50</sub> (μM)	Cli rat; hum <sup>d</sup> ml/min/g liver
		5-HT <sub>1A</sub> (I.A.)	5-HT <sub>1B</sub> (I.A.)	5-HT <sub>1D</sub> (I.A.)	hSerT	hERG		
17	NMe <sub>2</sub>	9.8 (0.0)	9.2 (0.0)	9.8 (0.0)	7.8	5.4	All > 10	0.5; 1.6
19	NHMe	9.8 (0.0)	8.9 (0.0)	9.9 (0.0)	7.5	<5.1	All > 9	<0.6; 1.3
20	NH <sub>2</sub>	9.5 (0.0)	8.8 (0.0)	9.8 (0.0)	7.5	4.5	All > 9	<0.8; 1.0
21		9.7 (0.0)	8.6 (0.0)	9.8 (0.0)	8.1	5.6	All > 8	<0.5; 1.7
22		9.9 (0.0)	9.3 (0.0)	10.4 (0.0)	7.8	6.2	All > 7	0.9; 1.4
23		9.8 (0.0)	9.2 (0.0)	10.0 (0.0)	7.7	6.3	2C19; 3	1.0; 2.7
24		9.6 (0.0)	8.7 (0.0)	9.8 (0.0)	8.0	6.7	NT	1.7; 3.1
25		9.9 (0.0)	8.8 (0.0)	10.7 (0.0)	8.3	6.7	All > 10	0.5; 2.8
26		9.8 (0.0)	8.8 (0.0)	9.7 (0.0)	8.2	6.3	2C19; 4	0.8; 2.3
27		9.9 (0.0)	9.0 (0.0)	9.8 (0.0)	7.9	5.9	All > 6	1.4; 1.8
28		9.4 (0.0)	8.8 (0.0)	9.8 (0.0)	8.0	6.0	All > 10	2.4; 5.8
29		9.4 (0.0)	9.0 (0.0)	9.8 (0.0)	7.3	4.5	All > 10	<0.5; 0.8

<sup>a</sup>Data from the agonist mode ( $pEC_{50}$ )<sup>\*</sup> are reported for those compounds with intrinsic activity (IA)  $\geq 0.4$  in this mode (i.e., partial or full agonists), whereas for those compounds with IA < 0.4 in the agonist mode (i.e., antagonists), data from the antagonist mode is reported ( $f$ - $pK_i$ ). See Experimental Section for assay details. <sup>b</sup>Each determination lies within 0.3 log units of the mean with a minimum of 3 replicates. See Experimental Section for assay details. <sup>c</sup>CYPEX assay: IC<sub>50</sub>  $\geq 5$  μM against different isoforms unless stated. See Experimental Section for assay details. <sup>d</sup>Intrinsic clearance in liver microsomes. See Experimental Section for assay details.

it had relatively modest hSerT affinity. The primary amide **20** also displayed a superb overall in vitro profile, comparable to that of **17** but with 10-fold reduced hERG affinity together with lower human intrinsic clearance.

On the basis of their outstanding in vitro profiles, **19**, **20**, and **29** were selected for further detailed characterization initially in rat PK studies (Table 5). Encouragingly, all three compounds showed good oral bioavailability and reduced blood clearance, relative to **17**, together with brain to blood ratios > 1 and high brain concentrations. The secondary amide **19** achieved the most impressive brain ratio (2.4), which may be due to the formation of an intramolecular H-bond between the amide NH and the imidazo nitrogen.<sup>16</sup> The availability of **19** allowed us to definitively confirm that this was a major metabolite produced from the *N*-dimethyl tertiary amide **17** both in vitro and in vivo (see above). In contrast, **19** was relatively metabolically stable to demethylation as evidenced by the detection of only minor traces of the corresponding primary amide **20** both in vitro and in vivo.

**Herg/QT risk.** Compounds **19**, **20**, and **29** were originally progressed on the basis of their low affinities for hERG channels as assessed by a dofetilide binding assay. To better

understand their relative cardiovascular safety profiles in terms of potential for QT interval prolongation, the effects of the compounds on human cardiac potassium channels stably expressed in HEK293 cells were investigated using a manual patch clamp electrophysiology assay.<sup>13</sup> The compounds inhibited hERG tail current with  $pIC_{50}$  values of 5.8, < 5.0, and 6.0, respectively, in broad agreement with dofetilide binding affinities. Compound **20** in particular demonstrated remarkably low inhibitory potency affording insufficient inhibition of hERG tail current at the highest concentration tested to allow IC<sub>50</sub> calculation ( $pIC_{25}$  ~6.2). Furthermore, when administered by iv infusion, **20** had no effect on QT interval duration in an anaesthetised guinea pig model<sup>17</sup> up to the maximum tested concentration of 7.7 μg/mL (solubility limited). Taken together, these data suggest that **20** possesses an excellent therapeutic index between biologically active concentrations (see below) and those likely to evoke QT prolongation via effects upon cardiac K<sup>+</sup> ion channels.

**DDI and Bioactivation Risk.** Although both **19** and **20** exhibited comparable direct inhibition profiles against the major human CYP450 enzymes during preliminary profiling (Table 4), different profiles emerged with respect to bioactivation and DDI



risk during further detailed CYP3A4 inhibition profiling in human liver microsomes using three different clinical probes (Table 6). The secondary amide **19** and the primary amide **20** both displayed a low potential for interacting with human CYP3A4, with **20** exhibiting the highest IC<sub>50</sub> values for all three probes (IC<sub>50</sub> > 88 μM). However, the results indicated a decrease in IC<sub>50</sub> values for the secondary amide **19** against the midazolam probe (IC<sub>50</sub> fold-change = 4) and the atorvastatin probe (IC<sub>50</sub> fold-change = 3), suggesting that **19** was a metabolism-dependent inhibitor of CYP3A4 for midazolam and atorvastatin in this assay. In contrast, the primary amide **20** gave no evidence of metabolism-dependent inhibition, up to 100 μM concentration.

To qualitatively access the risk of reactive metabolite formation, which is considered a risk factor for idiosyncratic toxicity, the propensity of **19** and **20** to form glutathione conjugates was also investigated.<sup>18</sup> Despite the closely related chemical structures, in the case of **19** a glutathione adduct (parent + GSH) was observed following incubation with GSH in the presence of human liver microsomes, with the bioactivation site determined to be the methyl amidic group. For the primary amide **20**, the same GSH conjugate could not be detected, highlighting a lower bioactivation risk relative to **19**. On the basis of its superior overall profile, **20** was selected for detailed in vitro and in vivo biological evaluation.

#### 5-HT<sub>1A/1B/1D</sub> Radioligand Binding and Functional Studies.

The affinities of **20** for human (h) recombinant 5-HT<sub>1</sub>

**Table 5.** Rat Pharmacokinetic Profile for Compounds<sup>a</sup>

compd	CL <sub>b</sub> <sup>b</sup> mL/min/kg	V <sub>ss</sub> L/kg	t <sub>1/2</sub> h	Fpo %	Br:Bl
<b>4</b>	8	3.4	5.2	63	0.7
<b>5</b>	29	1.7	1.0	26	1.5
<b>11</b>	12	1.6	1.8	51	0.5
<b>15</b>	10	7.1	8.7	43	2.7
<b>17</b>	29	3.5	2.1	50	1.8
<b>18</b>	10	3.9	5.1	48	1.6
<b>19</b>	8	3.8	6.3	104	2.4
<b>20</b>	10	2.9	4.4	45	1.1
<b>27</b>	20	5.0	3.1	43	3.2
<b>29</b>	12	5.5	7.6	65	1.7

<sup>a</sup>In vivo data determined by 0.5 mg/kg iv and 1 mg/kg po administration in rat. Br:Bl at 1 h following iv dosing. <sup>b</sup>Intrinsic clearance in liver microsomes.

**Table 6.** In Vitro Metabolism-Dependent Inhibition of Three Clinical Probes for Human CYP3A4 Using Human Liver Microsomes for Compounds **19** and **20**

clinical probe	<b>19</b>			<b>20</b>		
	initial IC <sub>50</sub> (μM)	final IC <sub>50</sub> (μM) <sup>a</sup>	fold-change	initial IC <sub>50</sub> (μM)	final IC <sub>50</sub> (μM) <sup>a</sup>	fold-change
midazolam	21	5	3.9	88	61	1.5
atorvastatin	8	3	2.7	100	100	1.0
nifedipine	100	82	1.4	100	100	1.0

<sup>a</sup>Following incubation.

**Table 7.** Summary of the Affinity (pK<sub>i</sub>) of **20** for Human Recombinant and Native Tissue 5-HT<sub>1A/1B/1D</sub> Receptors Determined Using Radioligand Binding (Mean ± SEM) and Human Functional Potency (pA<sub>2</sub>) Using [<sup>35</sup>S]-GTPγS-SPA Binding

	pK <sub>i</sub> for 5-HT <sub>1A/1B/1D</sub> receptors				
	rat <sup>a</sup>	guinea pig <sup>a</sup>	marmoset <sup>a</sup>	human <sup>b</sup>	human functional potency <sup>c</sup> pA <sub>2</sub>
5-HT <sub>1A</sub>	10.16 ± 0.14	10.24 ± 0.09	10.18 ± 0.12	9.94 ± 0.07	9.69 ± 0.18
5-HT <sub>1B</sub>	8.49 ± 0.03	9.80 ± 0.07	9.81 ± 0.13	9.10 ± 0.08	8.93 ± 0.05
5-HT <sub>1D</sub>				10.00 ± 0.08	9.77 ± 0.09

<sup>a</sup>Native tissue binding to 5-HT<sub>1A</sub> and 5-HT<sub>1B</sub> receptors in rat, guinea pig, and marmoset cortex using [<sup>3</sup>H]-WAY100635 and the 5-HT<sub>1D</sub> receptor antagonist radioligand [<sup>3</sup>H]-GR125743, respectively. <sup>b</sup>CHO cells expressing h5-HT<sub>1A</sub> or h5-HT<sub>1B</sub> or h5-HT<sub>1D</sub> receptors using [<sup>3</sup>H]-WAY100635 (5-HT<sub>1A</sub>) and [<sup>3</sup>H]-5-HT (5-HT<sub>1B</sub> and 5-HT<sub>1D</sub>). <sup>c</sup>[<sup>35</sup>S]-GTPγS-SPA binding to h5-HT<sub>1A</sub> (HEK), h5-HT<sub>1B</sub> (CHO) and h5-HT<sub>1D</sub> (CHO).

autoreceptors as assessed against Chinese hamster ovary (CHO) cells expressing h5-HT<sub>1A</sub> or h5-HT<sub>1B</sub> or h5-HT<sub>1D</sub> receptors using [<sup>3</sup>H]-WAY100635 (5-HT<sub>1A</sub>) and [<sup>3</sup>H]-5-HT (5-HT<sub>1B</sub> and 5-HT<sub>1D</sub>) were high and in good agreement with the functional potencies (Table 7). Comparable potencies were also obtained for native tissue 5-HT<sub>1A</sub> and 5-HT<sub>1B</sub> receptors in rat, guinea pig, and marmoset cortex using [<sup>3</sup>H]-WAY100635 and the 5-HT<sub>1B/1D</sub> receptor antagonist radioligand [<sup>3</sup>H]-GR125743, respectively. Under these conditions, 5-HT<sub>1D</sub> receptors are unlikely to contribute to the binding of [<sup>3</sup>H]-GR125743 due to their relatively low expression in this brain region.

In vitro determination of function using [<sup>35</sup>S]-GTPγS-SPA binding to h5-HT<sub>1A</sub> (HEK), h5-HT<sub>1B</sub> (CHO), and h5-HT<sub>1D</sub> (CHO) cell membranes was also assessed. Increasing concentrations of **20** produced parallel rightward-shift of the agonist (5-HT) concentration–response curves with the same maximal response in the presence and absence of the antagonist to afford pA<sub>2</sub> values in good agreement with the affinity constants (pK<sub>i</sub>) from receptor binding studies for all three receptors (Table 7). **20** alone did not stimulate [<sup>35</sup>S]-GTPγS binding at any of the receptors (at concentrations up to 1 μM), indicating that this compound does not have agonist properties at human recombinant 5-HT<sub>1A</sub>, 5-HT<sub>1B</sub>, and 5-HT<sub>1D</sub> receptors.

**Selectivity Profile.** Compound **20** displayed good selectivity (>100-fold) in a Cerep battery of more than 90 biological targets including GPCRs, ion channels, transporters, and enzymes with the exception of h-SERT and h-α<sub>1A</sub> adrenoceptors. Subsequently, **20** was determined to have a pK<sub>i</sub> values of 7.54 ± 0.07 (n = 3) and 8.56 ± 0.03 (n = 6) in h-SERT (ligand [<sup>3</sup>H]-citalopram) and h-α<sub>1A</sub> adrenoceptor (ligand [<sup>3</sup>H]-prazosin) filtration binding assays respectively.

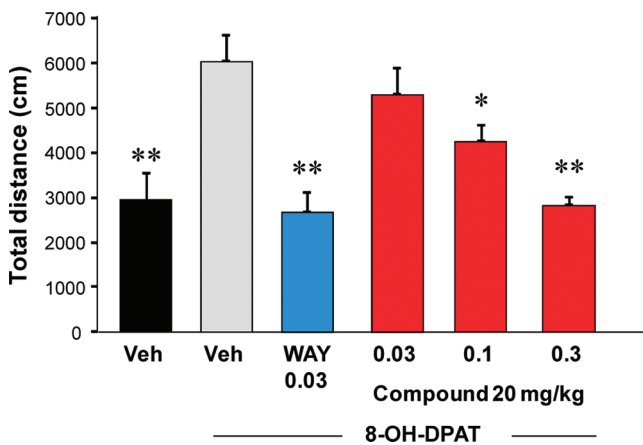


**Figure 2.** Effect of **20** on 8-OH-DPAT-induced hyperlocomotion in rat. Data represent mean ± SEM of 8 animals per group; \* *p* < 0.05, \*\* *p* < 0.01, ANOVA for completely randomized measures versus 8-OH-DPAT group, followed by Dunnett's test.

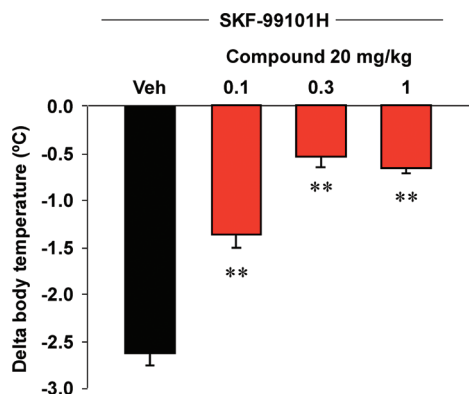


**Figure 3.** Effect of **20** on SKF-99101H-induced hypothermia in guinea pig. Data represent mean  $\pm$  SEM of 8 animals per group; \*\* =  $p < 0.01$ , ANOVA for completely randomized measures versus vehicle treated animals, followed by Dunnett's test.

**Table 8.** ED<sub>50</sub> and EC<sub>50</sub> for **20** in ex Vivo 5-HT<sub>1A</sub> and 5-HT<sub>1B</sub> Receptor Occupancy Studies in Guinea Pig Cortex

	ED <sub>50</sub> mg/kg	EC <sub>50</sub> ng/mL
5-HT <sub>1A</sub> ([ <sup>3</sup> H]-WAY100635 binding)	0.2	9.0
5-HT <sub>1B</sub> ([ <sup>3</sup> H]-GR125743 binding)	0.1	4.5

**In Vivo PD Profile.** Compound **20** was determined to have potent activity in both 5-HT<sub>1A</sub> and 5-HT<sub>1B</sub> agonist driven PD models in rat and guinea pig, respectively. In the 5-HT<sub>1A</sub> driven PD model,<sup>7b</sup> **20** significantly reversed 8-OH-DPAT-induced hyperlocomotion in rats in a dose-dependent manner (Figure 2), with an ED<sub>50</sub> of 0.05 mg/kg po (plasma EC<sub>50</sub> = 3.1 ng/mL). In the 5-HT<sub>1B</sub> driven PD model<sup>19</sup> **20** significantly reversed SKF-99101-induced hypothermia in the guinea pig in a dose dependent manner (Figure 3), with an ED<sub>50</sub> of 0.11 mg/kg po (extrapolated EC<sub>50</sub> = 2.3 ng/mL in plasma). In 5-HT<sub>1A</sub> and 5-HT<sub>1B</sub>, ex vivo receptor occupancy (RO) studies in guinea pig using [<sup>3</sup>H]-WAY100635 (5-HT<sub>1A</sub>) and [<sup>3</sup>H]-GR125743 (5-HT<sub>1B</sub>) as radioligands, compound **20** afforded ED<sub>50</sub> values of 0.2 and 0.1 mg/kg, respectively, (EC<sub>50</sub> 9.0 and 4.5 ng/g in cortex) which are in line with the above PD data (Table 8, Figure 4).

Evidence supporting fast-onset antidepressant/anxiolytic activity was obtained from both neurochemical studies and validated rodent and primate animal models of anxiety which will be the subject of a separate publication.

## Conclusions

In conclusion, the bioisosteric replacement of the metabolically labile *N*-methyl amide group of a series of benzoxazinones with small heterocyclic rings has led to novel series of fused tricyclic benzoxazines, many of which are potent 5-HT<sub>1A/B/D</sub> receptor antagonists both with and without concomitant hSerT activity. On the basis of their initial profiles fused imidazobenzoxazines (**6** and **10**) were selected for further exploration. Optimizing against multiple parameters in parallel identified several promising molecules which were progressed into more extensive characterization to enable the selection of the highest quality development candidate possible. In particular, **20** emerged as a potent 5-HT<sub>1A/B/D</sub> receptor antagonist with a high degree of selectivity over hERG potassium channels, favorable PK, and excellent activity in vivo in rodent PD models. On the basis of its outstanding overall profile, **20** was selected for progression as a clinical candidate with the ultimate aim to assess its potential as a

faster acting antidepressant/anxiolytic with reduced side-effect burden.

## Experimental Section

**Biological Test Methods. In Vitro Studies. a. Functional Potency: Primary Screen at Human Recombinant 5-HT<sub>1A</sub>, 5-HT<sub>1B</sub>, and 5-HT<sub>1D</sub> Receptors.** The functional potency of the compounds was determined by the following GTPγS binding assay. Cells used in the study are Chinese hamster ovary (CHO) cells and human embryo kidney (HEK293) cells transfected with DNA coding for human receptors as follows: HEK293\_5-HT<sub>1A</sub>, CHO\_5-HT<sub>1B</sub>, and CHO\_5-HT<sub>1D</sub>. Test compounds were initially dissolved in 100% dimethyl sulfoxide (DMSO) to a concentration of 10 mM. Serial dilution of the test compounds in 100% DMSO was carried out using a Biomek FX in 384 well assay plates so that the final top concentration of test compound was 3 μM in the assay. Test compounds were added at 1.0% total assay volume (TAV) to a solid, white, 384-well assay plate (Costar). Fifty percent TAV of precoupled (for 90 min at RT) membranes (5 μg/well), wheat-germ agglutinin polystyrene scintillation proximity assay beads (RPNQ0260 Amersham International) (0.25 mg/well) in 20 mM HEPES pH 7.4, 100 mM NaCl, 3 mM MgCl<sub>2</sub>, and 10 μM GDP were added. The third addition was a 20% TAV addition of either buffer (agonist format) or EC<sub>80</sub> of the agonist 5HT, prepared in assay buffer (antagonist format). The assay was started by the addition of 29% TAV of GTPγ[<sup>35</sup>S] 0.38 nM final (37 MBq/mL, 1160 Ci/mmol, Amersham). After all additions, assay plates were spun down for 1 min at 1000 rpm. Assay plates were counted on a Viewlux, 613/55 filter, for 5 min, between 2 and 6 h after the final addition.

**b. Receptor Affinities at Human Recombinant 5-HT<sub>1A</sub>, 5-HT<sub>1B</sub>, and 5-HT<sub>1D</sub> Receptors.** The affinities of the compounds for the human recombinant 5-HT<sub>1A</sub>, 5-HT<sub>1B</sub>, and 5-HT<sub>1D</sub> receptors were determined by the following assays. Cell pellets deriving from three clones of Chinese hamster ovary (CHO) cells stably transfected with the human 5-HT<sub>1A</sub>, 5-HT<sub>1B</sub>, and 5-HT<sub>1D</sub> receptors were resuspended in 10 volumes of 50 mM HEPES, 1 mM EDTA pH 7.4 in the presence of 1 μM leupeptin, 25 μg/mL bacitracin, 1 mM PMSF, and 2 μM pepstatin A (homogenization buffer). The cells were homogenized by a Glass Waring blender, and the resulting suspension spun at 500g for 20 min. The supernatant was then centrifuged at 48000g for 30 min and the final pellet was resuspended in homogenization buffer and homogenized again. The final suspension was distributed into aliquots and stored at -80 °C. Protein content in the membrane preparations was evaluated with BioRad protein assay. The day of the experiment, membrane aliquots were thawed and resuspended in Tris-Mg buffer (50 mM Tris/HCl, pH 7.7, 10 mM MgCl<sub>2</sub>, 1 g/L ascorbic acid, and 5 μMpargiline) and homogenized with Polytron immediately before use. Assays were performed into deep-well 96-well plates in a total volume of 0.5 mL/well. For 5-HT<sub>1A</sub> binding assay, 10 μg of protein of membranes were incubated with 0.5–1 nM [<sup>3</sup>H]-WAY100635 (TRK1034, 2.85 TBq/mmol, Amersham) and test drug, at 37 °C for 45 min, in Tris-Mg buffer supplemented with 30 μM GppNHp (guanosine 5'-[β,γ-imido]triphosphate). For 5-HT<sub>1B</sub> and 5-HT<sub>1D</sub> binding assays, 10 μg protein of membranes were incubated with 3 nM [<sup>3</sup>H]-5-HT (TRK1006, 4.00 TBq/mmol, Amersham) and test drug, at 37 °C for 45 min, in Tris-Mg buffer. Nonspecific binding (NSB) was defined using 10 μM of WAY100635 or 5-HT for 5-HT<sub>1A</sub> and 5-HT<sub>1B/D</sub>, respectively. Incubation was stopped by rapid filtration and washes with ice-cold 50 mM Tris buffer, pH 7.7, onto GF/B Unifilter plate (Perkin-Elmer) using a Perkin-Elmer Harvester. Radioactivity was measured by Topcount (Perkin-Elmer) scintillation counting. pK<sub>i</sub> values of test drugs were calculated according to the Cheng-Prusoff equation from the IC<sub>50</sub>, generated by an iterative least-squares curve fitting program (GraphPad Prism) and the K<sub>D</sub> (equilibrium dissociation constant of the radioligand) determined at each receptor type (5-HT<sub>1A</sub>, 5-HT<sub>1B</sub>, and 5-HT<sub>1D</sub>) through saturation experiments.

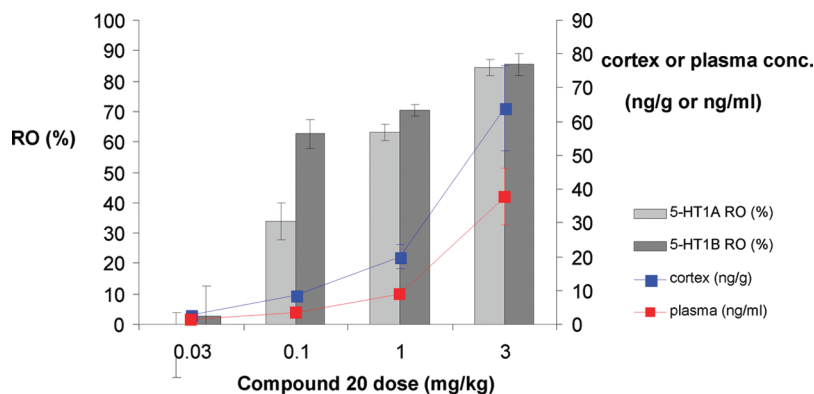


**Figure 4.** Occupancy at 5-HT<sub>1A</sub> and 5-HT<sub>1B</sub> receptors by **20** in guinea pig cortex together with brain and plasma exposure.

**c. Receptor Affinity at Native 5-HT<sub>1A</sub> and 5-HT<sub>1B/D</sub> Receptors Determined in Brain Cortex Tissue from Rat, Guinea Pig, and Marmoset.** Frozen brain cortex tissue samples from rat, guinea pig, and marmoset were thawed and resuspended in 20 volumes (v/w) of 50 mM Tris buffer, pH 7.7. Each tissue was homogenized with a Potter homogenizer and then spun at 48000g for 15 min. The pellet was resuspended in 20 volumes of 50 mM Tris buffer and homogenized with a Polytron homogenizer. The homogenate was incubated at 37 °C in a shaking water bath for 20 min. After a further homogenization, the tissue homogenate was centrifuged again at 48000g for 15 min. The supernatant was discarded, and the membrane pellet was finally resuspended in 4 volumes of 50 mM Tris buffer, distributed into tubes, and immediately frozen on dry ice and stored at -80 °C until use. Protein content was evaluated with BioRad protein assay.

The affinity of test compounds for 5-HT<sub>1A</sub> receptor in rat, guinea pig, and marmoset brain cortex was assessed through competition binding experiments using the 5-HT<sub>1A</sub>-selective antagonist radioligand [<sup>3</sup>H]-WAY100635 in low agonist affinity conditions, i.e. in the presence of 100 μM GPP(NH)p, a GTP analogue which promotes the transition of receptors to the inactive (G-protein uncoupled) state. Competition binding experiments were carried out in deep-well 96-plate format in a final volume of 0.5 mL/well of assay buffer (Tris 50 mM, pH 7.7 containing 0.2 mM ascorbic acid and 100 μM Gpp(NH)p) in the presence of 0.4–0.7 nM [<sup>3</sup>H]-WAY100635. NSB was determined in the presence of 10 μM WAY100635. The binding reaction was started through the addition of the membranes (~30–40 μg brain cortex membrane protein/well) and allowed to proceed for 45 min at 37 °C in a shaking water bath. At the end of the incubation, the reaction was stopped by filtration through glass fiber sheet (GF/C) presoaked in 0.3% PEI, followed by washes with ice cold 50 mM Tris buffer, pH 7.7, using a 96 way-harvester (Brandel M96/R). Radioactivity retained on the filters was determined by conventional liquid scintillation spectrometry.

The affinity of test compound for native 5-HT<sub>1B/D</sub> receptors in brain cortex was assessed through competition binding experiments essentially as described before but using the 5-HT<sub>1B/D</sub> antagonist radioligand [<sup>3</sup>H]-GR125743 (0.3 nM, TRK-1046, 2.96 TBq/mmol, Amersham) in an assay buffer containing: Tris 50 mM, pH 7.7, 10 mM MgCl<sub>2</sub>, 0.2 mM ascorbic acid, and 100 nM of a cocktail of four blockers (8-OH-DPAT, SB-243213, SB-258585, and SB-269970) of serotonergic receptors (5-HT<sub>1A</sub>, 5-HT<sub>2C</sub>, 5-HT<sub>6</sub>, and 5-HT<sub>7</sub>, respectively). NSB was determined in presence of 10 μM serotonin.

pK<sub>i</sub> value of the test drug was calculated according to the Cheng–Prusoff equation from the IC<sub>50</sub> and the K<sub>D</sub> determined in the three animal species evaluated (rat, guinea pig, and marmoset) through saturation experiments.

**d. [<sup>3</sup>H]Citalopram Binding Assay for Human Recombinant Serotonin Transporter (SERT).** The affinity of the compounds to bind the reuptake site of serotonin transporter (SERT) was

assessed by using [<sup>3</sup>H]citalopram binding assay performed in recombinant epithelial pig kidney cells stably transfected with human SERT (hSERT/LLCPK). Cell pellet was homogenized in 30–50 volumes of assay buffer (50 mM Tris, 120 mM NaCl, 5 mM KCl, 10 μM pargyline, 0.1% ascorbic acid, pH = 7.7) and centrifuged at 48000g for 20 min at 4 °C. The pellet was then resuspended in the same volume of assay buffer and after incubation at 37 °C for 20 min centrifuged as before. The final pellet was resuspended in assay buffer at ~0.2 mg protein/mL (as determined with BioRad protein assay).

The binding assay was performed in deep-well 96-well plate and the following additions were used up to a total assay volume of 400 μL: 100 μL of compound dilution or assay buffer (to define total binding, TB) or 10 μM fluoxetine (NSB), 100 μL of [<sup>3</sup>H]-citalopram (0.25 nM, TRK-1068, 296TBq/mmol, Amersham) and 200 μL of membranes diluted in assay buffer (2 μg of protein/well). Membranes were added last to initiate the reaction and incubated at room temperature for 2 h. The reaction was then stopped by rapid filtration through GF/B filter-plate (Unifilter, Perkin-Elmer), presoaked in 0.5% polyethylenimine (PEI) using a Perkin-Elmer harvester. Wells were washed three times with cold 0.9% NaCl solution. The dried plates were counted using TopCount (Perkin-Elmer) liquid scintillation counter.

pK<sub>i</sub> values were calculated according to the Cheng–Prusoff equation from the IC<sub>50</sub> and the K<sub>D</sub> determined at human SERT through saturation experiments.

**Receptor Selectivity.** The receptogram screen was performed by Cerep assessing the binding of 10 μM on 83 G-Protein coupled receptors, channels, enzymes, and transporters.

**hERG-[<sup>3</sup>H]-Dofetilide Binding Assay.** hERG activity was measured using [<sup>3</sup>H]-dofetilide binding in a scintillation proximity assay (SPA) format. The activity was measured with a PerkinElmer Viewlux imager.

**CYP450 Inhibition CYPEX Assay.** Inhibition (IC<sub>50</sub>) of human CYP1A2, 2C9, 2C19, 2D6, and 3A4 was determined using Cypex Bactosomes expressing the major human P450s. A range of concentrations (0.1, 0.2, 0.4, 1, 2, 4, and 10 μM) of test compound were prepared in methanol and preincubated at 37 °C for 10 min in 50 mM potassium phosphate buffer (pH 7.4) containing recombinant human CYP450 microsomal protein (0.1 mg/mL; Cypex Limited, Dundee, UK) and probe-fluorescent substrate. The final concentration of solvent was between 3 and 4.5% of the final volume. Following preincubation, NADPH regenerating system (7.8 mg glucose-6-phosphate, 1.7 mg NADP, and 6 units glucose-6-phosphate dehydrogenase/mL of 2% (w/v) NaHCO<sub>3</sub>; 25 μL) was added to each well to start the reaction. Production of fluorescent metabolite was then measured over a 10 min time-course using a Spectrafluor plus plate reader. The rate of metabolite production (AFU/min) was determined at each concentration of compound and converted to a percentage of the mean control rate using Magellan (Tecan software). The inhibition (IC<sub>50</sub>) of each compound was determined from the slope of the plot using Grafit v5 (Erithacus software, UK). Miconazole

was added as a positive control to each plate. CYP450 isoform substrates used were ethoxyresorufin (ER; 1A2; 0.5  $\mu\text{M}$ ), 7-methoxy-4-trifluoromethylcoumarin-3-acetic acid (FCA; 2C9; 50  $\mu\text{M}$ ), 3-butyryl-7-methoxycoumarin (BMC; 2C19; 10  $\mu\text{M}$ ), 4-methylaminomethyl-7-methoxycoumarin (MMC; 2D6; 10  $\mu\text{M}$ ), diethoxyfluorescein (DEF; 3A4; 1  $\mu\text{M}$ ), and 7-benzyloxyquinoline (7-BQ; 3A4; 25  $\mu\text{M}$ ). The test was performed in three replicates.

**CYP450 Inhibition Gentest Assay.** Inhibition potential ( $\text{IC}_{50}$ ) of test compound for inhibition of human CYP1A2, 2C9, 2C19, 2D6, and 3A4 was determined. A range of concentrations (0.1, 0.33, 1, 3.3, 10, 33, and 100  $\mu\text{M}$ ) of test compound prepared in methanol were preincubated at 37 °C for 10 min in 50 mM potassium phosphate buffer (pH 7.4) containing 0.1, 0.16, 0.2, or 0.4 mg recombinant human CYP450 microsomal protein  $\text{mL}^{-1}$  (Gentest Corporation, USA) and substrate. Following preincubation, 25  $\mu\text{L}$   $\text{mL}^{-1}$  of a NADPH regenerating system (7.8 mg glucose 6-phosphate, 1.7 mg NADP, and 6 U glucose-6-phosphate dehydrogenase  $\text{mL}^{-1}$  2% w/v  $\text{NaHCO}_3$ ) was added to each well to start the reaction. Production of fluorescent metabolite was then measured over a 10 min time-course using a Spectrafluor plus plate reader (Tecan). The rate of metabolite production (AFU/min) was determined for each concentration of compound and converted to a percentage of the mean control rate using Magellan v3.0 (Tecan software). The inhibitory potential ( $\text{IC}_{50}$ ) was determined from the slope of the plot using Grafit v4.12 (Erithacus software, UK). Miconazole was added as a positive control to each plate.

**CYP450 Inhibition Using Human Liver Microsomes.** A range of concentrations (0.1, 0.33, 1, 3.3, 10, 33, and 100  $\mu\text{M}$ ) of test compound were prepared in methanol. These were preincubated at 37 °C for 20 min in 50 mM potassium phosphate buffer (pH 7.4) containing pooled human liver microsomal protein (0.1 mg/mL; Xenotech) and CYP3A4 substrate (midazolam, atorvastatin or nifedipine; 2.5, 10, or 50  $\mu\text{M}$ , respectively). To start the reaction, NADPH regenerating system (7.8 mg glucose-6-phosphate, 1.7 mg NADP and 6 units glucose-6-phosphate dehydrogenase/mL of 2% (w/v)  $\text{NaHCO}_3$ ; 50  $\mu\text{L}/\text{mL}$ ) was added. Following a 5 min incubation, reactions were terminated with the addition of 250  $\mu\text{L}$  acetonitrile.

Quantification of 1'-hydroxy midazolam, *o*-hydroxy atorvastatin, and oxidized nifedipine metabolites was carried out using validated HPLC-MS analytical methods. Inhibition ( $\text{IC}_{50}$ ) was determined using Grafit (Erithacus software, UK).

**Metabolism-Dependent Inhibition of CYP3A4 in Human Liver Microsomes.** A range of concentrations (0.1, 0.33, 1, 3.3, 10, 33, and 100  $\mu\text{M}$ ) of the test compound and troleanomycin (positive control) were prepared in methanol. These were pre-incubated at 37 °C for 20 min in 50 mM potassium phosphate buffer (pH 7.4) containing pooled human liver microsomal protein (0.1 mg/mL; Xenotech) and NADPH regenerating system (7.8 mg glucose-6-phosphate, 1.7 mg NADP, and 6 units glucose-6-phosphate dehydrogenase/mL of 2% (w/v)  $\text{NaHCO}_3$ ; 50  $\mu\text{L}/\text{mL}$ ) [Cofactor preincubation samples] or CYP3A4 substrate (midazolam, atorvastatin, or nifedipine; 2.5, 10, or 50  $\mu\text{M}$ , respectively) [substrate preincubation samples]. To start the reaction, CYP3A4 substrate (midazolam, atorvastatin, or nifedipine; 2.5, 10, or 50  $\mu\text{M}$ , respectively) was added to the cofactor preincubation samples and NADPH regenerating system (50  $\mu\text{L}/\text{mL}$ ) to the substrate preincubation samples. Following 5 min incubation for midazolam and 10 min incubation for atorvastatin or nifedipine, reactions were terminated with the addition of 250  $\mu\text{L}$  of acetonitrile.

Quantification of 1'-hydroxy midazolam, *o*-hydroxy atorvastatin and oxidized nifedipine metabolites was carried out using validated HPLC-MS analytical methods. Inhibition ( $\text{IC}_{50}$ ) was determined using Grafit (Erithacus software, UK) and TDI assessed comparing the difference in  $\text{IC}_{50}$  between the cofactor and substrate preincubation samples for each CYP3A4 substrate.

**GSH Trapping.** Incubations were carried out with human liver microsomes (1 mg/mL), glutathione (10 mM),  $\text{MgCl}_2$  (3 mM), NADPH generating system (7.8 mg glucose-6-phosphate, 1.7 mg

NADP, 6 U glucose-6-phosphate dehydrogenase per mL of 2% sodium bicarbonate), one positive substrate (acetaminophen). Test compound and acetaminophen as positive control were incubated at 100  $\mu\text{M}$  at 37 °C for 1.5 h. Incubation mixtures were collected at 0 and 90 min and quenched with 6% acetic acid in acetonitrile. Assay mixtures were centrifuged (900g, 10 min, 4 °C), and 10  $\mu\text{L}$  of the resulting supernatants were injected into the HPLC-MS system.

**Intrinsic Clearance (CLi) Assay.** Intrinsic clearance (CLi) values were determined in rat and human liver microsomes. Test compounds (0.5  $\mu\text{M}$ ) were incubated at 37 °C for 30 min in 50 mM potassium phosphate buffer (pH 7.4) containing 0.5 mg microsomal protein/mL. The reaction was started by addition of cofactor (NADPH; 8 mg/mL). The final concentration of solvent was 1% of the final volume. At 0, 3, 6, 9, 15, and 30 min, an aliquot (50  $\mu\text{L}$ ) was taken, quenched with acetonitrile containing an appropriate internal standard, and analyzed by HPLC-MS/MS. The intrinsic clearance (CLi) was determined from the first-order elimination constant by nonlinear regression using Grafit v5 (Erithacus software, UK), corrected for the volume of the incubation, and assuming 52.5 mg microsomal protein/g liver for all species. Values for CLi were expressed as mL/min/g liver. The lower limit of quantification of clearance was determined to be when < 15% of the compound had been metabolized by 30 min and this corresponded to a CLi value of 0.5 mL/min/g liver. The upper limit was 50 mL/min/g liver.

**Patch Clamp hERG Electrophysiology Assay.** On the days of experimentation, a weighed amount of the test substance was formulated in dimethyl sulfoxide (DMSO; lot no. U10781; Sigma-Aldrich, UK), by shaking, to give a stock concentration of 10 mM of the test compound. The 10 mM stock solution was serially diluted in DMSO to give further stock solutions of 1 and 0.1 mM. Aliquots of these stock solutions were added to bath solution to achieve final perfusion concentrations of 0.1, 1, and 10  $\mu\text{M}$  test compound. The corresponding vehicle concentration in all test substance perfusion solutions was 0.1% DMSO. Test substance stock formulations were freshly prepared on each day of experimentation, stored at room temperature, and protected from light.

**Reference Substance.** E-4031 (batch no. MLE9446; Wako Pure Chemical Industries Ltd.). Stock solutions of E-4031 (100  $\mu\text{M}$ ) were prepared in reverse osmosis water, aliquoted, and stored at approximately -20 °C until use. On the day of use, the 100  $\mu\text{M}$  stock solution was added to bath solution to give a final perfusion concentration of 100 nM.

**Bath and Pipette Solutions.** The composition of bath solution was (mM): NaCl 137, KCl 4,  $\text{CaCl}_2$  1.8,  $\text{MgCl}_2$  1.0, D-glucose 10, *N*-2-hydroxyethylpiperazine-*N'*-2-ethanesulfonic acid (HEPES) 10, pH 7.4 with 1 M NaOH. Pipette solution was prepared in batches, aliquoted, and stored frozen until the day of use. The composition of pipet solution was (mM): KCl 130,  $\text{MgCl}_2$  1.0, ethylene glycol-bis(ss-aminoethyl ether)-*N,N,N',N'*-tetraacetic acid (EGTA) 5, MgATP 5, HEPES 10, pH 7.2 with 1 M KOH.

**Study Design.** Cells (passage number: 48) were transferred to the recording chamber and continuously perfused (at approximately 1–2 mL/min) with bath solution at room temperature. High resistance seals (seal resistances > 1.5 G $\Omega$ ) were formed between the patch electrodes (resistance range: 1.4–5.5 M $\Omega$ ) and individual cells. The membrane across the electrode tip was then ruptured and the whole-cell patch-clamp configuration was established. Once a stable patch had been achieved, recording commenced in voltage-clamp mode, with the cell initially clamped at -80 mV. Currents were evoked by stepping the membrane potential to +20 mV and then to -50 mV (tail current). Test compound at 10, 1, and 0.1  $\mu\text{M}$  was used to produce (if any) inhibition of hERG tail current and therefore to investigate the concentration–response relationship ( $n = 3$  cells/concentration). The effect of the vehicle (0.1% DMSO) was investigated in three cells. The effect of 100 nM E-4031 was investigated in two of the vehicle treated cells to confirm the sensitivity of the test system to

an agent known to block hERG current. All perfusion solutions were applied for approximately 10 min.

**In Vivo Studies.** All experimental procedures were carried out in accordance with Italian law (Legislative Decree no. 116, 27 January 1992), which acknowledges the European Directive 86/609/EEC and were fully compliant with GlaxoSmithKline policy and codes of practice on the care and use of laboratory animals. Animals were housed under standard laboratory conditions ( $23 \pm 1^\circ\text{C}$ ; lights on 0600–1800 h) with food and water ad libitum.

**8-OH-DPAT-Induced Hyperlocomotion.**<sup>20</sup> Male Sprague–Dawley rats (250–350 g, Charles River, Italy) were used. Rat locomotory activity was assessed as the total distance (cm) traveled by each rat in the test arena over a 30 min period using Digiscan analyzer system (Omnitech, model RXYZCM-8, Columbus, OH). Rats were placed individually into clear plexiglas boxes, measuring 40 cm  $\times$  40 cm  $\times$  30.5 cm and covered with a perforated plexiglas lid. Infrared monitoring sensors were located around the perimeter walls. Data were collected and analyzed by a Digiscan analyzer (Omnitech, model DCM-4, Columbus, OH), which in turn transferred information to a computer. Total distance was recorded during 30 min test period.

The animals were treated orally with vehicle or compound **20** at 0.03, 0.1, or 0.3 mg/kg 120 min before a subcutaneous (sc) injection of 0.2 mg/kg of 8-OH-DPAT. The standard 5-HT<sub>1A</sub> receptor antagonist WAY-100,635 (Fletcher, 1996) was used as positive control (0.03 mg/kg sc 30 min before test).

**SKF99101H-Induced Hypothermia.** Male Dunkin Hartley guinea pigs (300–400 g, Harlan, Germany) were used. Core body temperature was monitored on freely moving animals by using a telemetric transponders (IPTT-200 BioMedic Data System, Seaford, DE) implanted sc in the dorso-cervical area four days before test. Body temperature was recorded by placing the scanner (DAS 5007 BioMedic Data System, Seaford, DE) above the transponder until a stable reading was achieved.

The animals were treated orally with vehicle or compound **20** at 0.1, 0.3, or 1 mg/kg 60 min before sc administration of 10 mg/kg of SKF-99101H a standard 5-HT<sub>1/7</sub> agonist. Temperature measurements were taken immediately prior to SKF-99101H dosing (time 0) and every 30 min for a total of 180 min. Data are expressed as a fall in the peak temperature ( $^\circ\text{C}$ ) compared to body temperature at time 0 (just before SKF-99101H administration).

**Drugs.** Compound **20** was suspended in Methocel 0.5% (w/v, HPCM Colorcon, Dow Chemical Company, Midland, MI). 8-OH-DPAT was purchased by Sigma (Italy) and dissolved in saline before use. WAY-100,635 (*N*-{2-[4-(2-methoxyphenyl)-1-piperazinyl]ethyl}-*N*-(2-pyridinyl) cyclohexane-carboxamide trihydrochloride) was synthesized in house and dissolved in sterile water before use. SKF-99101H (3-2-dimethylaminoethyl-4-chloro-5-propoxyindole hemifumarate) was synthesized in house and dissolved in saline before use. All compounds were prepared with correction for salt form such that doses cited refer to mg/kg of active principle.

**Measurement of the Occupancy at 5-HT<sub>1A</sub> and 5-HT<sub>1B/D</sub> Receptors Using ex Vivo Binding on Guinea Pig Brain Cortex Homogenate.** The test compound was dissolved in 0.5% methocel and administered per os (po) to male guinea pigs (about 250 g, strain DH, Harlan), dosed at 0.03, 0.1, 1, and 3 mg/kg po; a further group was run with vehicle. For each dose condition, four animals were used. The receptor occupancy determination was performed 1 h after the administration. Animals were sacrificed by decapitation, and the brain was quickly removed and the cerebral cortex was dissected. One-fourth of the tissue was used by the DMPK Department for the analytical quantification of the amount of the test compound in the cortex. Remaining tissue was processed for binding experiments. The cortex sample from each single animal of the different experimental groups was weighed and homogenized in 30 mL of 50 mM Tris Buffer pH 7.7 using a glass–glass Potter

homogenizer. The homogenate was diluted to a final volume of 100-fold the original wet weight of tissue and further homogenized by using a Polytron homogenizer. The resulting homogenate was directly used for the 5-HT<sub>1B/D</sub> binding, while for 5-HT<sub>1A</sub> binding it was further diluted 1:1. For each cortex sample, the protein concentration was determined by using the Bio-Rad Protein Assay. Occupancy of 5-HT<sub>1A</sub> and 5-HT<sub>1B/D</sub> receptors was assessed through binding experiments using [<sup>3</sup>H]-WAY100635 and [<sup>3</sup>H]-GR125743, as described previously.

Each single animal of the different groups (vehicle and compound-treated) generated from each binding assay four values: two total bound (TB) and two nonspecific bound (NSB). The average of the NSB was subtracted from the TB of each brain sample to obtain the specific binding (SB). Maximal SB values were from the vehicle-treated animals and SB gradually decreased in the drug-treated animals with the increase of the dose. Percentage of specific binding in drug-treated animals (% SB) was then calculated and the % of receptor occupancy (RO) inversely correlates with the % SB (i.e., 0% RO is in the vehicle group and 100% RO is when the drug completely blocks the radioligand binding). The ED<sub>50</sub> values were estimated by nonlinear regression between % RO and the dose of compound administered. EC<sub>50</sub>s were estimated using % RO vs compound concentration in the brain or in the plasma, as analytically determined by DMPK.

**Anesthetized Guinea Pig Model for the Assessment of QT Prolongation.** Prior to the experiment, six male Hartley guinea pigs (Charles River, France), weighing between 564 and 605 g on the day of the test, were anaesthetised with urethane (1–1.5 g/kg ip), tracheotomized, artificially ventilated with a tidal volume of approximately 1 mL/100 g at a rate of 54 cycles/min, and surgically prepared for the experiment (i.e., insertion of catheters in appropriate blood vessels, see below, and placement of surface electrodes for lead II electrocardiogram recording). The animal's temperature was kept constant between 36.8 and 38.0  $^\circ\text{C}$ . Once physiological parameters were stabilized (approximately 30 min following surgery), each animal was given either the vehicle (5% w/v dextrose in aqueous 0.9 w/v sodium chloride) or test compound by the intravenous route (via the jugular vein) over 15 min/treatment. The following parameters were recorded: arterial pressure (via the carotid artery), heart rate, electrocardiography (i.e., RR, PQ, QRS, and QT interval duration; the QT interval was corrected for heart rate changes according to Fridericia, Bazett and Van de Water's formula). Parameters were recorded prior to dosing to establish baseline measurements and continuously during the infusion period but data were reported every 5 min during each infusion period. In addition, blood samples (0.3 mL) were collected via the femoral artery at the end of each infusion period for toxicokinetic evaluations.

**In Vivo Pharmacokinetics in Rat.** The pharmacokinetics and oral bioavailability of test compounds were determined following iv (bolus) and po administration to male Sprague–Dawley rats of the at 0.5 and 1 mg free base/kg, respectively. Blood samples were assayed for test compound concentration using a method based on protein precipitation followed by HPLC-MS/MS analysis.

**Chemistry. General Methods.** Proton magnetic resonance (NMR) spectra were recorded either on Varian instruments at 300, 400, or 500 MHz, or on a Bruker instrument at 300 MHz. Chemical shifts are reported in ppm ( $\delta$ ) using the residual solvent line as internal standard. Splitting patterns are designed as s, singlet; d, doublet; t, triplet; q, quartet; m, multiplet; b, broad. The NMR spectra were recorded at a temperature ranging from 25 to 90  $^\circ\text{C}$ . When more than one conformer was detected, the chemical shifts for the most abundant one is reported. Mass spectra (MS) are typically taken on a 4 II triple quadrupole mass spectrometer (Micromass UK) or on a Agilent MSD 1100 mass spectrometer, operating in ES (+) and ES (–) ionization mode or on an Agilent LC/MSD 1100 mass spectrometer, operating in ES (+) and ES (–) ionization mode coupled with HPLC instrument

Agilent 1100 series. LC/MS-ES (+): analysis performed on a Supelcosil ABZ +Plus (33 mm × 4.6 mm, 3 μm) (mobile phase: 100% [water + 0.1% HCO<sub>2</sub>H] for 1 min, then from 100% [water + 0.1% HCO<sub>2</sub>H] to 5% [water + 0.1% HCO<sub>2</sub>H] and 95% [CH<sub>3</sub>CN] in 5 min, finally under these conditions for 2 min; T = 40 °C; flux = 1 mL/min; LC/MS-ES (-): analysis performed on a Supelcosil ABZ +Plus (33 mm × 4.6 mm, 3 μm) (mobile phase: 100% [water + 0.05% NH<sub>3</sub>] for 1 min, then from 100% [water + 0.05% NH<sub>3</sub>] to 5% [water + 0.05% NH<sub>3</sub>] and 95% [CH<sub>3</sub>CN] in 5 min, finally under these conditions for 2 min; T = 40 °C; flux = 1 mL/min]; in the mass spectra, only one peak in the molecular ion cluster is reported.

DAD chromatographic traces, mass chromatograms, and mass spectra were taken on a UPLC/MS Acquity™ system coupled with a Micromass ZQTM mass spectrometer operating in ESI positive or negative. The phases used are: (A) H<sub>2</sub>O/ACN 95/5 + 0.1% TFA; (B) H<sub>2</sub>O/ACN 5/95 + 0.1% TFA. The gradient was: (*t* = 0 min) 95%A 5%B, (*t* = 0.25) 95%A 5%B, (*t* = 3.30) 100%B, (*t* = 4.0) 100%B, followed by 1 min of reconditioning. Flash silica gel chromatography was carried out on silica gel 230–400 mesh (supplied by Merck AG Darmstadt, Germany) or over Varian Mega Be–Si prepacked cartridges or over prepacked Biotage silica cartridges. SPE-SCX cartridges are ion exchange solid phase extraction columns supplied by Varian. The eluent used with SPE-SCX cartridges is methanol followed by 2N ammonia solution in methanol. In a number of preparations, purification was performed using either Biotage manual flash chromatography (Flash+) or automatic flash chromatography (Horizon, SP1) systems. All these instruments work with Biotage Silica cartridges. SPE-Si cartridges are silica solid phase extraction columns supplied by Varian. Microwave reactions were carried out in a Personal Chemistry Emrys Optimiser (300 W). All reactions were carried out under anhydrous nitrogen or argon atmosphere using standard Schlenk techniques. Most chemicals and solvents were analytical grade and used without further purification.

The purity of the compounds reported in the manuscript was established through HPLC methodology. All the compounds reported in the manuscript have a purity >95%.

**General Synthetic Procedures.** The preparation of compounds 6–29 are shown in Schemes 1–6. Experimental and analytical data for compounds 6, 10, 11–13, and 19–20 are described below.

**8-(2-Propen-1-yl)-2H-1,4-benzoxazine-3(4H)-thione (31).** A mixture of 8-(2-propen-1-yl)-2H-1,4-benzoxazin-3(4H)-one **30** (2 g, 10.5 mmol) and Lawesson's reagent (2.2 g, 5.3 mmol) in dry toluene (35 mL) was heated at reflux for 1 h. The mixture was cooled to room temperature and the solvent evaporated in vacuo. The crude material was purified by chromatography on silica gel eluting with 10% cyclohexane in AcOEt to afford the title compound (1.9 g, 88%) as a white solid. <sup>1</sup>H NMR (300 MHz, CDCl<sub>3</sub>) δ: 9.6 (s, 1H), 6.85 (m, 2H), 6.75 (m, 1H), 5.8 (m, 1H), 5.05 (m, 2H), 4.75 (s, 2H), 3.35 (d, 2H).

**3-(Methylthio)-8-(2-propen-1-yl)-2H-1,4-benzoxazine (32).** To a mixture of intermediate **31** (100 mg, 0.49 mmol) and KOH (69 mg, 1.23 mmol) in acetone (2 mL) was added methyl iodide (46 μL, 0.74 mmol) in two portions 15 min apart. The reaction mixture was heated under reflux for 2 h, cooled, filtered to remove KI, and evaporated in vacuo. The crude material was purified by chromatography on silica gel eluting with 10% cyclohexane in AcOEt to afford the title compound (70 mg, 65%) as a colorless oil. <sup>1</sup>H NMR (300 MHz, CDCl<sub>3</sub>) δ: 7.2 (m, 1H), 6.9 (bs, 2H), 5.9 (m, 1H), 5 (m, 2H), 4.5 (s, 2H), 3.3 (d, 2H), 2.5 (s, 3H). MS: *m/z* 220.2 [M + H]<sup>+</sup>.

**N-[2,2-Bis(methoxy)ethyl]-8-(2-propen-1-yl)-2H-1,4-benzoxazin-3-amine (33).** A mixture of intermediate **32** (180 mg, 0.82 mmol) and aminoacetaldehyde dimethylacetal (134 μL, 1.23 mmol) in dry EtOH (5 mL) was heated at reflux for 9 h. The volatiles were evaporated in vacuo and the crude product was purified by chromatography on silica gel eluting with 40%

AcOEt in cyclohexane to afford the title compound (93 mg, 41%) as a colorless oil. <sup>1</sup>H NMR (300 MHz, CDCl<sub>3</sub>) δ: 7.2 (m, 1H), 6.9 (bs, 2H), 5.9 (m, 1H), 5 (m, 2H), 4.5 (s, 2H), 3.3 (d, 2H), 2.5 (s, 3H). MS: *m/z* 277.3 [M + H]<sup>+</sup>.

**6-(2-Propen-1-yl)-4H-imidazo[2,1-*c*][1,4]benzoxazine (34).** A mixture of intermediate **33** (90 mg, 0.33 mmol) and conc HCl (0.8 mL) in MeOH (1 mL) was heated at reflux for 3 h. After concentration in vacuo the residue was dissolved in CH<sub>2</sub>Cl<sub>2</sub> (20 mL), washed with an aqueous saturated solution of NaHCO<sub>3</sub> (15 mL), dried over Na<sub>2</sub>SO<sub>4</sub>, and evaporated in vacuo. The crude material was purified by chromatography on silica gel eluting with 35% AcOEt in cyclohexane to afford the title compound (65 mg, 92%) as a yellow solid. <sup>1</sup>H NMR (300 MHz, CDCl<sub>3</sub>) δ: 7.4 (bs, 1H), 7.2 (bs, 2H), 7.05 (bs, 2H), 5.95 (m, 1H), 5.3 (s, 2H), 5.1 (m, 2H), 3.45 (d, 2H). MS: *m/z* 213.3 [M + H]<sup>+</sup>.

**4H-Imidazo[2,1-*c*][1,4]benzoxazin-6-ylacetaldehyde (35).** 4-Methylmorpholine *N*-oxide (218 mg, 1.87 mmol) and osmium tetroxide (225 μL of a 4% by wt solution in water, 0.035 equiv) were added to a solution of intermediate **34** (200 mg, 0.94 mmol) in a 8:1 mixture of acetone/water (17.5 mL). The reaction was left under stirring overnight before additional osmium tetroxide (200 μL, 0.03 equiv) and 4-methylmorpholine *N*-oxide (250 mg, 2.1 mmol) were added to drive the reaction to completion. After a further 24 h, the reaction was quenched with a saturated aqueous solution of sodium sulfite (75 mL). After 30 min stirring, the mixture was extracted with AcOEt (3 × 75 mL) and the combined organic layers were dried over Na<sub>2</sub>SO<sub>4</sub> and concentrated in vacuo to give a 7:3 mixture (by NMR) of the desired product **35** and 4H-imidazo[2,1-*c*][1,4]benzoxazine-6-carbaldehyde, which was used without purification in the next step.

**4H-Imidazo[2,1-*c*][1,4]benzoxazin-6-ylacetaldehyde 35.** <sup>1</sup>H NMR (300 MHz, CDCl<sub>3</sub>) δ: 9.8 (s, 1H), 7–7.4 (m, 5H), 5.25 (s, 2H), 3.8 (s, 2H). MS *m/z* 215.3 [M + H]<sup>+</sup>.

**4H-Imidazo[2,1-*c*][1,4]benzoxazine-6-carbaldehyde.** <sup>1</sup>H NMR (300 MHz, CDCl<sub>3</sub>) δ: 10.5 (s, 1H), 7.7 (m, 1H), 7.5 (m, 1H), 7–7.4 (m, 3H), 5.4 (s, 2H). MS *m/z* 201.3 [M + H]<sup>+</sup>.

**6-[2-[4-(2-Methyl-5-quinolinyl)-1-piperazinyl]ethyl]-4H-imidazo[2,1-*c*][1,4]benzoxazine Dihydrochloride (6).** 2-Methyl-5-piperazin-1-yl-quinoline (68 mg, 0.25 mmol) was added to a 7:3 mixture of intermediate **35** and 4H-imidazo[2,1-*c*][1,4]benzoxazine-6-carbaldehyde (50 mg, 0.2 mmol) in dry 1,2-dichloroethane (5 mL) at room temperature. After 15 min, sodium triacetoxyborohydride (52 mg, 0.25 mmol) was added and the resulting reaction mixture was stirred for 3 h, then quenched with a saturated aqueous solution of NH<sub>4</sub>Cl (20 mL) and extracted with CH<sub>2</sub>Cl<sub>2</sub> (3 × 20 mL). The combined organics were dried over Na<sub>2</sub>SO<sub>4</sub> and concentrated in vacuo. The crude products were separated by chromatography on silica gel eluting with 2% MeOH in CH<sub>2</sub>Cl<sub>2</sub> to afford the free base of the title compound (14 mg; 20% yield) and the byproduct 6-{{[4-(2-methyl-5-quinolinyl)-1-piperazinyl]methyl}-4H-imidazo[2,1-*c*][1,4]benzoxazine (14 mg, 50% yield). The free base of **6** was dissolved in dry MeOH (0.5 mL), and HCl (2.2 equiv of a 1.25 M solution in methanol) was slowly added at 0 °C. The resulting suspension was stirred at 0 °C for 4 h, followed by evaporation of the volatiles and trituration with Et<sub>2</sub>O to give the title compound as a yellow solid. <sup>1</sup>H NMR (500 MHz, DMSO-*d*<sub>6</sub>) δ: 11.07 (bs, 1H), 8.78 (m, 1H), 8.05 (s, 1H), 7.88 (m, 2H), 7.7 (m, 2H), 7.38 (m, 1H), 7.25 (bs, 1H), 7.24 (d, 1H), 7.18 (t, 1H), 5.43 (s, 2H), 3.8–3.2 (m, 12H), 2.84 (s, 3H). MS *m/z* 426.3 [M + H]<sup>+</sup>.

**6-{{[4-(2-Methyl-5-quinolinyl)-1-piperazinyl]methyl}-4H-imidazo[2,1-*c*][1,4]benzoxazine dihydrochloride.** <sup>1</sup>H NMR (500 MHz, DMSO-*d*<sub>6</sub>) δ: 10.64 (bs, 1H), 8.8 (bs, 1H), 8.0 (m, 1H), 7.9 (bs, 3H), 7.8 (bs, 1H), 7.7 (d, 1H), 7.1–7.4 (m, 3H), 5.5 (s, 2H), 4.5 (s, 2H), 3.8–3.1 (m, 8H), 2.7 (s, 3H). MS *m/z*: 412.4 [M + H]<sup>+</sup>.

**Ethyl 6-(2-Propen-1-yl)-4H-imidazo[5,1-*c*][1,4]benzoxazine-3-carboxylate (47).** Diethyl chlorophosphate (0.15 mL, 1.8 mmol) was added to a solution of intermediate **30** (170 mg, 0.9 mmol) and potassium *t*-butoxide (110 mg, 0.9 mmol) in dry DMF (5 mL) at 0 °C. After 10 min, a solution of ethyl isocyanacetate (0.15 mL, 1.35 mmol) and potassium *t*-butoxide (152 mg, 1.35 mmol) in dry

DMF (2 mL) was added. The reaction mixture was stirred at 60 °C for 6 h and then cooled and quenched with water (5 mL). The DMF was evaporated in vacuo and the crude product purified by SPE-SI cartridge eluting with 30% AcOEt in cyclohexane to afford the title compound (132 mg, 52%) as a white solid. <sup>1</sup>H NMR (300 MHz, CDCl<sub>3</sub>) δ: 8.2 (s, 1H), 7.55 (d, 1H), 7.3 (d, 1H), 7.2 (t, 1H), 6.25 (m, 1H), 5.7 (s, 2H), 5.2–5.3 (m, 2H), 4.65 (q, 2H), 3.65 (d, 2H), 1.6 (t, 3H). MS *m/z* 285.2 [M + H]<sup>+</sup>.

**Ethyl 6-(2-Oxoethyl)-4H-imidazo[5,1-*c*][1,4]benzoxazine-3-carboxylate (51).** Intermediate **47** (77 mg, 0.27 mmol) was treated with osmium tetroxide according to the general procedure described for **38** (D28) to afford the title compound (52 mg, 67%) as a white solid. <sup>1</sup>H NMR (300 MHz, CDCl<sub>3</sub>) δ: 9.8 (s, 1H), 8 (s, 1H), 7.4 (t, 1H), 7–7.1 (m, 2H), 5.5 (s, 2H), 4.35 (q, 2H), 3.8 (s, 2H), 1.4 (t, 3H).

**Ethyl 6-(2-[4-(2-Methyl-5-quinolinyl)-1-piperazinyl]ethyl)-4H-imidazo[5,1-*c*][1,4]benzoxazine-3-carboxylate (14).** A mixture of intermediate **51** (D6) (50 mg, 0.17 mmol) was reacted with 2-methyl-5-piperazin-1-yl-quinoline (58 mg, 0.21 mmol) as in the general procedure described for **6** of to afford the free base of the title compound (61 mg, 70%) as a white solid. <sup>1</sup>H NMR (300 MHz, CDCl<sub>3</sub>) δ: 8.4 (d, 1H), 8 (s, 1H), 7.7 (d, 1H), 7.55 (t, 1H), 7.3 (d, 1H), 7.2 (m, 1H), 7.1 (d, 1H), 6.95–7.05 (m, 2H), 5.55 (s, 2H), 4.4 (q, 2H), 2.7–3.15 (m, 12H), 3.7 (s, 3H), 1.4 (t, 3H). MS *m/z* 498.5 [M + H]<sup>+</sup>.

The free base (20 mg, 0.04 mmol) was dissolved in dry MeOH (1 mL) and treated with HCl (0.068 mL of a 1.25N solution in MeOH, 0.084 mmol) at 0 °C. The resulting suspension was stirred at 0 °C for 4 h. Evaporation of the volatiles and trituration with Et<sub>2</sub>O gave the dihydrochloride of the title compound (20 mg, 87%) as a yellow solid. <sup>1</sup>H NMR (500 MHz, DMSO-*d*<sub>6</sub>) δ: 10.67 (bs, 1H), 8.8–8.6 (bs, 1H), 7.89 (dd, 1H), 7.82 (s, 2H), 7.64 (bs, 1H), 7.35 (s, 1H), 7.29 (dd, 1H), 7.2 (d, 1H), 4.3 (q, 2H), 3.76 (dd, 2H), 3.6–3.3 (m, 8H), 2.8 (s, 3H), 1.33 (t, 3H).

**6-(2-Propen-1-yl)-4H-imidazo[5,1-*c*][1,4]benzoxazine-3-carboxylic Acid (48).** A solution of intermediate **47** (900 mg, 3.17 mmol) in a 1:1 mixture of MeOH and 1 M solution of NaOH (60 mL) was stirred at 60 °C for 30 min. The cooled reaction mixture was neutralized with AcOH and then cooled to 0 °C. The crude product was collected by filtration, washed with MeOH, and dried to afford the title compound (570 mg, 70%) as a white solid. <sup>1</sup>H NMR (300 MHz, CDCl<sub>3</sub>) δ: 8.55 (s, 1H), 7.75 (d, 1H), 7.05–7.15 (m, 2H), 5.8 (m, 1H), 5.5 (s, 2H), 5.0–5.1 (m, 2H), 3.45 (d, 2H).

**6-(2-Propen-1-yl)-4H-imidazo[5,1-*c*][1,4]benzoxazine (49).** A mixture of intermediate **48** (120 mg, 0.47 mmol) in 1,2-dichlorobenzene (1.5 mL) was irradiated in a microwave reactor (300 W, 250 °C, 10 min). The solvent was removed by SPE-SCX cartridge (eluting with MeOH followed by 2N ammonia solution in MeOH) to afford the title compound (61 mg, 100%) as a white solid. <sup>1</sup>H NMR (300 MHz, CDCl<sub>3</sub>) δ: 8.6 (s, 1H), 7.6 (d, 1H), 7.2–7.35 (m, 3H), 6.25 (m, 1H), 5.5 (s, 2H), 5.35 (m, 2H), 3.65 (d, 2H). MS *m/z* 213.2 [M + H]<sup>+</sup>.

**4H-Imidazo[5,1-*c*][1,4]benzoxazin-6-ylacetaldehyde (50).** The title compound was prepared in 30% yield according to the general oxidation procedure described for **38** starting from intermediate **49** (60 mg, 0.28 mmol). <sup>1</sup>H NMR (300 MHz, CDCl<sub>3</sub>) δ: 9.8 (s, 1H), 8.15 (s, 1H), 7.7 (d, 1H), 7.3–7.45 (m, 3H), 5.5 (s, 2H), 3.75 (s, 2H).

**6-(2-[4-(2-Methyl-5-quinolinyl)-1-piperazinyl]ethyl)-4H-imidazo[5,1-*c*][1,4]benzoxazine Dihydrochloride (10).** The title compound was prepared in 40% yield following the general reductive amination procedure described for **6** starting from intermediate **50** (20 mg, 0.08 mmol) and 2-methyl-5-piperazin-1-yl-quinoline (20 mg, 0.1 mmol). <sup>1</sup>H NMR (500 MHz, DMSO-*d*<sub>6</sub>) δ: 10.64 (bs, 1H), 8.64 (s, 1H), 8.47 (d, 1H), 7.81 (d, 1H), 7.7 (s, 2H), 7.48 (d, 1H), 7.3–7.1 (m, 3H), 7.07 (s, 1H), 5.35 (s, 2H), 3.8–3.1 (m, 12H), 2.68 (s, 3H). MS *m/z* 426.3 [M + H]<sup>+</sup>.

**6-(2-[4-(2-Methyl-5-quinolinyl)-1-piperazinyl]ethyl)-4H-imidazo[5,1-*c*][1,4]benzoxazine-3-carboxylic Acid (65).** To a solution of compound **14** (220 mg, 0.44 mmol) in MeOH (3 mL) was added

NaOH (3 mL of a 10% aq solution), and the resulting white suspension was heated for 5 min under microwave irradiation at 120 °C. The resulting pale-yellow solid was filtered off, suspended in water (15 mL), and the solution was neutralized with an aqueous solution of AcOH. The resulting off-white solid precipitate was filtered and washed with Et<sub>2</sub>O (3 × 20 mL) affording the title compound (0.168 g, 81%). <sup>1</sup>H NMR (300 MHz, DMSO-*d*<sub>6</sub>) δ: 8.49 (bs, 1H), 8.3 (d, 1H), 7.7 (d, 1H), 7.55 (bs, 1H), 7.35 (d, 1H), 7.2 (d, 1H), 7.07 (m, 2H), 5.5 (s, 2H), 3.05–2.75 (m, 15H). MS *m/z* 470.3 [M + H]<sup>+</sup>.

**6-(2-[4-(2-Methyl-5-quinolinyl)-1-piperazinyl]ethyl)-4H-imidazo[5,1-*c*][1,4]benzoxazine-3-carboxamide Dihydrochloride (20).** To a stirred solution of compound **65** (30 mg, 0.06 mmol) and DIPEA (0.012 mL) in DMF (1 mL) was added TBTU (22.6 mg, 0.07 mmol), and the resulting solution was stirred for 1 h at room temperature. Hexamethyldisilazane (0.013 mL, 0.07 mmol) was added and the solution stirred for 1 h. The excess of amine was scavenged by using a PS-isocyanate resin, and after filtration of the resin and evaporation of the solvent, the crude product was purified by SPE cartridge (silica gel) eluting with 3% MeOH in CH<sub>2</sub>Cl<sub>2</sub> to afford the free base of the title compound as a white solid. The free base was dissolved in dry MeOH and treated with HCl (2.1 equiv of 1N solution in Et<sub>2</sub>O) at 0 °C. Evaporation of solvent and trituration with Et<sub>2</sub>O gave the final compound (22 mg, 65%). <sup>1</sup>H NMR (300 MHz, DMSO-*d*<sub>6</sub>) δ: 11.4 (bs, 1H), 9.05 (d, 1H), 8.59 (s, 1H), 8.08 (d, 1H), 8.01 (t, 1H), 7.91 (d, 1H), 7.84 (dd, 1H), 7.51–7.49 (bd, 2H), 7.33 (bs, 1H), 7.26 (d, 1H), 7.15 (t, 1H), 5.59 (s, 2H), 3.81–3.72 (bd, 2H), 3.53–3.49 (bd, 4H), 3.43–3.39 (bd, 4H), 3.22–3.17 (m, 2H), 2.97 (s, 3H). MS *m/z* 469.4 [M + H]<sup>+</sup>.

**General Procedure for Amide Formation (19, 21–23 and 25–29).** To a stirred solution of intermediate **65** (1 equiv) and DIPEA (1.1 equiv) in DMF was added TBTU (1.1 equiv) and the resulting solution was stirred for 1 h at room temperature. The desired amine (1.1 equiv) was added and the solution stirred for 1 h. The crude solution was applied to a SPE-SCX cartridge (eluting with MeOH followed by 2N ammonia solution in MeOH). After evaporation of solvent from the ammonia fractions and trituration with Et<sub>2</sub>O, the free base of the desired compound was isolated in pure form. The free base was dissolved in dry MeOH and treated with HCl (2.1 equiv of 1N solution in Et<sub>2</sub>O) at 0 °C. Evaporation of solvent and trituration with Et<sub>2</sub>O gave the final compounds in pure form.

***N*-Methyl-6-(2-[4-(2-methyl-5-quinolinyl)-1-piperazinyl]ethyl)-4H-imidazo[5,1-*c*][1,4]benzoxazine-3-carboxamide Dihydrochloride (19).** The title compound was prepared in 44% yield from intermediate **65** following the general procedure for amide formation using methylamine (2N solution in THF). <sup>1</sup>H NMR (300 MHz, DMSO-*d*<sub>6</sub>) δ: 11.29 (bs, 1H), 9.05 (d, 1H), 8.60 (s, 1H), 8.07–7.97 (m, 2H), 7.89 (d, 1H), 7.83 (dd, 1H), 7.49 (d, 1H), 7.37 (bs, 1H), 7.24 (t, 1H), 7.15 (t, 1H), 5.59 (s, 2H), 3.70–3.38 (m, 10H), 3.22–3.15 (m, 2H), 2.96 (s, 3H), 2.74 (d, 3H). MS *m/z* 483.4 [M + H]<sup>+</sup>.

**1-Methyl-6-(2-propen-1-yl)-4H-[1,2,4]triazolo[3,4-*c*][1,4]benzoxazine (55).** A solution of intermediate **31** (1.38 g, 6.71 mmol) in absolute EtOH (50 mL) was added dropwise over 1 h to a solution of hydrazine monohydrate (8 mL) in absolute EtOH (50 mL) at 80 °C. The resulting reaction mixture was stirred at reflux for a further 40 min and concentrated in vacuo to afford (3*E*)-8-(2-propen-1-yl)-2*H*-1,4-benzoxazin-3(4*H*)-one hydrazone **54**, which was immediately used in the following step without purification. The hydrazone **54** was mixed with trimethyl orthoacetate (15 mL) and heated with stirring at 150 °C for 10 min under microwave irradiation. The resulting reaction mixture was evaporated in vacuo and purified by flash chromatography on silica gel, eluting with 5% MeOH in CH<sub>2</sub>Cl<sub>2</sub> to give the title compound (0.78 g, 51%) as a pale-yellow solid. <sup>1</sup>H NMR (300 MHz, CDCl<sub>3</sub>) δ: 7.36 (d, 1H), 7.11–7.03 (m, 2H), 6.01–5.84 (m, 1H), 5.25 (s, 2H), 5.08–5.01 (m, 2H), 3.43 (d, 2H), 2.76 (s, 3H). MS *m/z* 228.20 [M + H]<sup>+</sup>.

**(1-Methyl-4*H*-[1,2,4]triazolo[3,4-*c*][1,4]benzoxazin-6-yl)acetaldehyde (56).** Intermediate **55** (D24) (142 mg, 0.62 mmol) was

treated with 4-methylmorpholine *N*-oxide (145 mg, 1.24 mmol) and osmium tetroxide (0.20 mL of 4% by wt solution in water) according to the procedure described for **53a** to give the title compound (50 mg, 35%) as a white solid which was used without further purification. <sup>1</sup>H NMR (300 MHz, CDCl<sub>3</sub>) δ: 9.78 (s, 1H), 7.49 (d, 1H), 7.15–7.12 (m, 2H), 5.28 (s, 2H), 3.82 (s, 2H), 2.79 (s, 3H). MS *m/z* 230.20 [M + H]<sup>+</sup>.

**1-Methyl-6-{2-[4-(2-methyl-5-quinolinyl)-1-piperazinyl]ethyl}-4H-[1,2,4]triazolo[3,4-*c*][1,4]benzoxazine dihydrochloride (11).** The title compound was prepared in 71% yield following the general reductive amination procedure described for **6** starting from intermediate **56** (45 mg, 0.2 mmol) and 2-methyl-5-piperazin-1-yl-quinoline (54 mg, 0.24 mmol). <sup>1</sup>H NMR (500 MHz, DMSO-*d*<sub>6</sub>) δ: 11.21 (bs, 1H), 8.92 (bs, 1H), 7.97 (bs, 2H), 7.81 (bd, 1H), 7.72 (d, 1H), 7.45 (bd, 1H), 7.34 (d, 1H), 7.25 (t, 1H), 5.46 (s, 2H), 3.75 (d, 2H), 3.3–3.6 (m, 8H), 3.24 (m, 2H), 2.91 (s, 3H), 2.74 (s, 3H). MS *m/z* 441.3 [M + H]<sup>+</sup>.

**6-(2-Propen-1-yl)-4H-tetrazolo[5,1-*c*][1,4]benzoxazine (57).** A solution of hydrazine hydrate (380 μL, 12.2 mmol) in dry THF (2 mL) was treated dropwise with a solution of intermediate **31** (500 mg, 2.44 mmol) in THF (25 mL) at 20 °C. After stirring for 1.5 h, the solvent was removed under reduced pressure to afford the intermediate hydrazone **54**, which was used in the following step without any further purification. To a suspension of hydrazone **54** (495 mg, 2.44 mmol) in 0.5N HCl (15 mL), a solution of NaNO<sub>2</sub> (252 mg, 3.66 mmol) in water (2 mL) was added dropwise at 5 °C. After stirring for 4 h, the mixture was neutralized with a saturated aqueous solution of NaHCO<sub>3</sub> and extracted with CH<sub>2</sub>Cl<sub>2</sub> (3 × 30 mL). The combined organic layers were dried over Na<sub>2</sub>SO<sub>4</sub> and concentrated in vacuo. The crude product was purified by flash chromatography on silica gel eluting with 20% EtOAc in cyclohexane to afford the title compound (235 mg, 45%). <sup>1</sup>H NMR (400 MHz, CDCl<sub>3</sub>) δ: 7.85 (d, 1H), 7.28–7.16 (m, 2H), 6.01–5.94 (m, 1H), 5.65 (s, 2H), 5.14–5.08 (m, 2H), 3.47 (d, 2H). MS *m/z* 215.10 [M + H]<sup>+</sup>.

**4H-Tetrazolo[5,1-*c*][1,4]benzoxazin-6-ylacetaldehyde (58).** The title compound was prepared following the procedure of **38** from intermediate **57** (235 mg, 1.09 mmol). The crude product was purified by flash chromatography on silica gel eluting with AcOEt/cyclohexane (4/6) to afford the title compound (144 mg, 61%). <sup>1</sup>H NMR (300 MHz, CDCl<sub>3</sub>) δ: 3.77 (s, 2H) 5.56 (s, 2H) 7.14 (d, 2H) 7.90 (t, 1H) 9.72 (s, 1H).

**6-[2-[4-(2-Methyl-5-quinolinyl)-1-piperazinyl]ethyl]-4H-tetrazolo[5,1-*c*][1,4]benzoxazine Dihydrochloride (13).** The title compound was prepared in 77% yield following the general reductive amination procedure described for **6** starting from intermediate **58** (47 mg, 0.218 mmol) and 2-methyl-5-(1-piperazinyl)quinoline (74 mg, 0.326 mmol). The crude product was purified by flash chromatography on silica gel eluting with 2% MeOH in CH<sub>2</sub>Cl<sub>2</sub> to afford the free base of the title compound (72 mg, 77%). Treatment with HCl (2.2 equiv of 1.25 M solution in MeOH) in 2:1 MeOH/CH<sub>2</sub>Cl<sub>2</sub> (3 mL) at 0 °C gave the title compound as a yellow solid. <sup>1</sup>H NMR (500 MHz, DMSO-*d*<sub>6</sub>) δ: 2.72 (s, 3H) 3.18–3.56 (m, 10H) 3.66–3.78 (m, 2H) 5.84–5.97 (m, 2H) 7.22–7.32 (m, 2H) 7.43 (d, 1H) 7.47–7.63 (m, 1H) 7.67–7.83 (m, 2H) 7.89 (dd, 1H) 8.36–8.75 (m, 1H) 11.24 (bs, 1H). MS *m/z* 428.00 [M + H]<sup>+</sup>.

**2-(2-Butyn-1-yloxy)-1-nitro-3-(2-propen-1-yl)benzene (60).** A mixture of 2-nitro-6-(2-propen-1-yl)phenol **59** (500 mg, 2.79 mmol), 1-bromo-2-butyne (269 μL, 3.07 mmol, 1.1 equiv), and K<sub>2</sub>CO<sub>3</sub> (424 mg, 3.07 mmol, 1.1 equiv) in acetone (20 mL) was heated at reflux for 4 h. The mixture was cooled to room temperature before the solids were filtered off and washed with acetone (30 mL). The combined organics were concentrated in vacuo, and the crude product was purified by flash chromatography on silica gel eluting with 10% AcOEt in cyclohexane to afford the title compound (640 mg, 99%). <sup>1</sup>H NMR (300 MHz, CDCl<sub>3</sub>) δ: 7.65 (m, 1H), 7.39 (m, 1H), 7.13 (m, 1H), 5.90 (m, 1H), 5.11–5.02 (m, 2H), 4.60 (m, 2H), 3.49 (m, 2H), 1.77 (s, 3H).

**[2-(2-Butyn-1-yloxy)-3-(2-propen-1-yl)phenyl]amine (61).** To a solution of intermediate **60** (640 mg, 2.77 mmol) in glacial

AcOH (10 mL) was added iron powder (619 mg, 11.1 mmol, 4 equiv) at room temperature and the mixture was stirred for 16 h. The solvent was evaporated in vacuo, and AcOEt (50 mL) was added to the residue. The precipitate was removed by filtration, and the filtrate was extracted successively with 1N NaOH (10 mL) and brine (10 mL) before drying over MgSO<sub>4</sub> and evaporation in vacuo to afford the title compound (540 mg, 97%). <sup>1</sup>H NMR (300 MHz, CDCl<sub>3</sub>) δ: 6.86 (m, 1H), 6.61–6.53 (m, 2H), 5.94 (m, 1H), 5.10–5.01 (m, 2H), 4.44 (m, 2H), 3.82 (bs, 2H), 3.40 (m, 2H), 1.87 (m, 3H). MS *m/z* 202.10 [M + H]<sup>+</sup>.

**1-Azido-2-(2-butyn-1-yloxy)-3-(2-propen-1-yl)benzene (62).** A solution of NaNO<sub>2</sub> (72 mg, 1.05 mmol, 1.05 equiv) in water (1 mL) was added dropwise to a suspension of intermediate **61** (201 mg, 1 mmol) in 4N HCl (3 mL) under vigorous stirring and ice/water cooling. The mixture was then neutralized by addition of aqueous NaHCO<sub>3</sub>, and a solution of sodium azide (65 mg, 1 mmol, 1 equiv) in water (1 mL) was slowly added at 5 °C. After 30 min, the mixture was extracted with Et<sub>2</sub>O (3 × 20 mL) and the combined organics dried over MgSO<sub>4</sub> and evaporated under reduced pressure to give the title azide (222 mg, 98%), which was used for the next step without further purification. <sup>1</sup>H NMR (300 MHz, CDCl<sub>3</sub>) δ: 7.02 (m, 1H), 6.96–6.87 (m, 2H), 5.90 (m, 1H), 5.10–4.95 (m, 2H), 4.55 (s, 2H), 3.45 (m, 2H), 1.80 (s, 3H).

**3-Methyl-6-(2-propen-1-yl)-4H-[1,2,3]triazolo[5,1-*c*][1,4]benzoxazine (63).** A solution of intermediate **62** (222 mg, 0.98 mmol) in toluene (8 mL) was heated at reflux for 2.5 h. The solvent was then evaporated under reduced pressure, and the residue was purified by flash chromatography on silica gel eluting with 20% AcOEt in cyclohexane to afford the title compound (183 mg, 82%). <sup>1</sup>H NMR (300 MHz, CDCl<sub>3</sub>) δ: 7.86 (m, 1H), 7.10–7.00 (m, 2H), 5.90 (m, 1H), 5.25 (s, 2H), 5.05–4.98 (m, 2H), 3.39 (m, 2H), 2.33 (s, 3H). MS *m/z* 228.20 [M + H]<sup>+</sup>.

**(3-Methyl-4H-[1,2,3]triazolo[5,1-*c*][1,4]benzoxazin-6-yl)acetaldehyde (64).** The title compound was prepared in 66% yield according to the procedure of intermediate **38** starting from intermediate **63** (183 mg, 0.806 mmol). The product was purified by flash chromatography on silica gel using AcOEt/cyclohexane (2/3) as eluent. <sup>1</sup>H NMR (300 MHz, CDCl<sub>3</sub>) δ: 9.72 (s, 1H), 7.97 (m, 1H), 7.1 (m, 2H), 5.26 (s, 2H), 3.74 (s, 2H), 2.33 (s, 3H). MS *m/z* 230.10 [M + H]<sup>+</sup>.

**3-Methyl-6-{2-[4-(2-methyl-5-quinolinyl)-1-piperazinyl]ethyl}-4H-[1,2,3]triazolo[5,1-*c*][1,4]benzoxazine dihydrochloride (12).** The title compound was prepared in 81% yield following the general reductive amination procedure described for **6** starting from intermediate **64** (60 mg, 0.262 mmol). The crude product was purified by flash chromatography on silica gel eluting with a gradient of 1–3% MeOH in CH<sub>2</sub>Cl<sub>2</sub> to afford the free base of the title compound (93 mg, 81%). Treatment with HCl (2.2 equiv of 1.25N solution in MeOH) in 4:1 MeOH/CH<sub>2</sub>Cl<sub>2</sub> (5 mL) at 0 °C gave the title compound as a solid. <sup>1</sup>H NMR (500 MHz, DMSO-*d*<sub>6</sub>) δ: 10.51 (bs, 1H), 8.62 (bs, 1H), 7.93 (d, 1H), 7.78 (bs, 2H), 7.60 (bs, 1H), 7.37 (d, 1H), 7.32 (bs, 1H), 7.24 (t, 1H), 5.58 (s, 2H), 3.75–3.10 (m, 12H), 2.76 (s, 3H), 2.34 (s, 3H). MS *m/z* 441.20 [M + H]<sup>+</sup>.

**Acknowledgment.** We thank Dr. Carla Marchioro and her analytical group for the high quality support received and all other colleagues who helped in generating the data reported in this manuscript.

**Supporting Information Available:** Experimental and supporting data for compounds **7–9**, **15–18**, and **21–29**. This material is available free of charge via the Internet at <http://pubs.acs.org>.

## References

- (1) (a) Hirschfeld, R. M. A. History and evolution of the monoamine hypothesis of depression. *J. Clin. Psychiatry* **2000**, *61* (Suppl. 6), 4–6. (b) Lucki, I. The spectrum of behaviors influenced by serotonin.



- Biol. Psychiatry* **1998**, *44*, 151–162. (c) Naughton, M.; Mulrooney, J. B.; Leonard, B. E. A review of the role of serotonin receptors in psychiatric disorders. *Human Psychopharmacol.* **2000**, *15*, 397–415.
- (2) Vaswani, M.; Linda, F. K.; Ramesh, S. Role of selective serotonin reuptake inhibitors in psychiatric disorders: a comprehensive review. *Prog. Neuro-Psychopharm. Biol. Psychiatry* **2003**, *27*, 85–102.
- (3) (a) Wood, M. D.; Thomas, D. R.; Watson, J. M. Therapeutic potential of serotonin antagonists in depressive disorders. *Exp. Opin. Invest. Drugs* **2002**, *11*, 457–467. (b) Blier, P.; De Montigny, C. Serotonin and drug-induced therapeutic responses in major depression, obsessive-compulsive and panic disorders. *Neuropsychopharmacology* **1999**, *21*, 91–98S.
- (4) Beyer, C. E.; Boikess, S.; Luo, B.; Dawson, L. A. Comparison of the effects of antidepressants on norepinephrine and serotonin concentrations in the rat frontal cortex: an in vivo microdialysis study. *J. Psychopharm.* **2002**, *16*, 297–304.
- (5) Roberts, C.; Price, G. W.; Middlemiss, D. N. Ligands for the investigation of 5-HT autoreceptor function. *Brain Res. Bull.* **2001**, *56*, 463–469.
- (6) (a) Dawson, L. A.; Hughes, Z. A.; Watson, J. M.; Arban, R.; Price, G. W. 5-HT autoreceptors: Pharmacological tools and therapeutic potential. *Curr. Top. Pharmacol.* **2004**, *8*, 251–264. (b) Dawson, L. A.; Bromidge, S. M. 5-HT<sub>1</sub> receptor augmentation strategies as enhanced efficacy therapeutics for psychiatric disorders. *Curr. Top. Med. Chem.* **2008**, *8*, 1008–1023.
- (7) (a) Atkinson, P. J.; Bromidge, S. M.; Duxon, M. S.; Gaster, L. M.; Hadley, M. S.; Hammond, B.; Johnson, C. N.; Middlemiss, D. N.; North, S. E.; Price, G. W.; Rami, H. K.; Riley, G. J.; Scott, C. M.; Shaw, T. E.; Starr, K. R.; Stemp, G.; Thewlis, K. M.; Thomas, D. R.; Thompson, M.; Vong, A. K. K.; Watson, J. M. 3,4-Dihydro-2H-benzoxazinones are 5-HT<sub>1A</sub> receptor antagonists with potent 5-HT reuptake inhibitory activity. *Bioorg. Med. Chem. Lett.* **2005**, *15*, 737–741. (b) Hughes, Z. A.; Starr, K. R.; Scott, C. M.; Newson, M. J.; Sharp, T.; Watson, J. M.; Hagan, J. J.; Dawson, L. A. Simultaneous blockade of 5-HT<sub>1A/B</sub> receptors and 5-HT transporters results in acute increases in extracellular 5-HT in both rats and guinea pigs: in vivo characterization of the novel 5-HT<sub>1A/B</sub> receptor antagonist/5-HT transport inhibitor SB-649915-B. *Psychopharmacology* **2007**, *192*, 121–133. (c) Lovell, P. J.; Blaney, F. E.; Goodacre, C. J.; Scott, C. M.; Smith, P. W.; Starr, K. R.; Thewlis, K. M.; Vong, A. K. K.; Ward, S. E.; Watson, J. M. 3,4-Dihydro-2H-benzoxazinones as dual-acting 5-HT<sub>1A</sub> receptor antagonists and serotonin reuptake inhibitors. *Bioorg. Med. Chem. Lett.* **2007**, *17*, 1033–1036. (c) Ward, S. E.; Johnson, C. N.; Lovell, P. J.; Scott, C. M.; Smith, P. W.; Stemp, G.; Thewlis, K. M.; Vong, A. K.; Watson, J. M. Studies on a series of potent, orally bioavailable, 5-HT<sub>1</sub> receptor ligands. *Bioorg. Med. Chem. Lett.* **2007**, *17*, 5214–5217.
- (8) (a) Serafinowska, H. T.; Blaney, F. E.; Lovell, P. J.; Merlo, G.; Scott, C. M.; Smith, P. W.; Starr, K. R.; Watson, J. M. Novel 5-HT<sub>1A/1B/1D</sub> receptors antagonists with potent 5-HT reuptake inhibitory activity. *Bioorg. Med. Chem. Lett.* **2008**, *18*, 5581–5585. (b) Bromidge, S. M.; Bertani, B.; Borriello, M.; Faedo, S.; Gordon, L. J.; Granci, E.; Hill, M.; Marshall, H. R.; Stasi, L. P.; Zucchelli, V.; Merlo, G.; Vesentini, A.; Watson, J. M.; Zonzini, L. 6-[2-(4-Aryl-1-piperazinyl)ethyl]-2H-1,4-benzoxazin-3(4H)-ones: dual-acting 5-HT<sub>1</sub> receptor antagonists and serotonin reuptake inhibitors. *Bioorg. Med. Chem. Lett.* **2008**, *18*, 5653–5656.
- (9) Bromidge, S. M.; Bertani, B.; Borriello, M.; Bozzoli, A.; Faedo, S.; Gianotti, M.; Gordon, L. J.; Hill, M.; Zucchelli, V.; Watson, J. M.; Zonzini, L. 8-[2-(4-Aryl-1-piperazinyl)ethyl]-2H-1,4-benzoxazin-3(4H)-ones: dual-acting 5-HT<sub>1</sub> receptor antagonists and serotonin reuptake inhibitors, part II. *Bioorg. Med. Chem. Lett.* **2009**, *19*, 2338–2342.
- (10) Bartsch, H.; Erker, T.; Neubauer, G. Studies on the chemistry of 1,4-oxazines. 18. Synthesis of tricyclic 1,4-benzoxazines via nucleophilic substitution of activated precursors. *J. Heterocycl. Chem.* **1989**, *26*, 205–207.
- (11) Rudorf, W. D.; Janietz, D. Intramolecular 1,3-dipolar cycloadditions of aryl azides with alkynyl substituents. *J. Prakt. Chem.* **1987**, *329*, 55–61.
- (12) (a) Sanguinetti, M. C.; Tristani-Firouzi, M. hERG potassium channels and cardiac arrhythmia. *Nature* **2006**, *440* (7083), 463–469. (b) Mitcheson, J. S. hERG Potassium Channels and the Structural Basis of Drug-Induced Arrhythmias. *Chem. Res. Toxicol.* **2008**, *21*, 1005–1010.
- (13) Aptuit Limited, 3 Simpson Parkway, Livingston, West Lothian, EH54 7BH, Scotland, www.apuit.uk.
- (14) Shamovsky, I.; Connolly, S.; David, L.; Ivanova, S.; Nordén, B.; Springthorpe, B.; Urbahns, K. Overcoming Undesirable hERG Potency of Chemokine Receptor Antagonists Using Baseline Lipophilicity Relationships. *J. Med. Chem.* **2008**, *51*, 1162–1178.
- (15) Huang, S.; Strong, J. M.; Zhang, L.; Reynolds, K. S.; Nallani, S.; Temple, R.; Abraham, S.; Al Habet, S.; Baweja, R. K.; Burckart, G. J.; Chung, S.; Colangelo, P.; Frucht, D.; Green, M. D.; Hepp, P.; Karnaukhova, E.; Ko, H.; Lee, J.; Marroum, P. J.; Norden, J. M.; Qiu, W.; Rahman, A.; Sobel, S.; Stifano, T.; Thummel, K.; Wei, X.; Yasuda, S.; Zheng, J. H.; Zhao, H.; Lesko, L. J. New era in drug interaction evaluation: US Food and Drug Administration update on CYP enzymes, transporters, and the guidance process. *J. Clin. Pharm.* **2008**, *48*, 662–670.
- (16) Ashwood, V. A.; Field, M. J.; Horwell, D. C.; Julien-Larose, C.; Lewthwaite, R. A.; McCleary, S.; Pritchard, M. C.; Raphy, J.; Singh, L. Utilization of an intramolecular hydrogen bond to increase the CNS penetration of an NK(1) receptor antagonist. *J. Med. Chem.* **2001**, *44*, 2276–2285.
- (17) Centre de Recherches Biologiques, CERB, Chemin de Montfort, 18800 Bougy, France, www.cerb.fr.
- (18) Gan, J.; Ruan, Q.; He, B.; Zhu, M.; Shyu, W. C.; Humphreys, W. G. In vitro screening of 50 highly prescribed drugs for thiol adduct formation—comparison of potential for drug-induced toxicity and extent of adduct formation. *Chem. Res. Toxicol.* **2009**, *22*, 690–698.
- (19) Hagan, J. J.; Slade, P. D.; Gaster, L.; Jeffrey, P.; Hatcher, J. P.; Middlemiss, D. N. Stimulation of 5-HT<sub>1B</sub> receptors causes hypothermia in the guinea pig. *Eur. J. Pharmacol.* **1997**, *331*, 169–174.
- (20) Fletcher, A.; Forster, E. A.; Bill, D. J.; Brown, G.; Cliffe, I. A.; Hartley, J. E.; Jones, D. E.; McLenachan, A.; Stanhope, K. J.; Critchley, D. J. P.; Childs, K. J.; Middlefell, V. C.; Lanfumey, L.; Corradetti, R.; Laporte, A.; Gozlan, H.; Hamon, M.; Dourish, C. T. Electrophysiological, biochemical, neurohormonal and behavioural studies with WAY-100635, a potent, selective and silent 5-HT<sub>1A</sub> receptor antagonist. *Behav. Brain Res.* **1996**, *73*, 337–353.